Research Square

Preprints are preliminary reports that have not undergone peer review.
They should not be considered conclusive, used to inform clinical practice,
or referenced by the media as validated information.

Transferable integrative and conjugative element ICEtea carrying multidrug resistance genes in bovine mastitis- associated Streptococcus uberis

Thamonwan Wanganuttara
Okayama University
Hidehito Matsui
Kitasato University
Iyo Takemura-Uchiyama
Okayama University
Jumpei Uchiyama
uchiyama@okayama-u.ac.jp

Okayama University
Takuya Yagisawa
Hokkaido Agriculture Mutual Aid Association
Naoki Suzuki
Hiroshima University
Shoji Ogino
Nippon Zenyaku Kogyo Co., Ltd.
Toshihiro Tsukui
Nippon Zenyaku Kogyo Co., Ltd.
Poowadon Muenraya
Okayama University
Hironobu Murakami
Azabu University
Hideharu Hagiya
Okayama University

Article

Keywords: antimicrobial resistance (AMR), bovine mastitis, integrative and conjugative element (ICE), One Health, Streptococcus agalactiae, Streptococcus uberis

Posted Date: September 17th, 2026

DOI: https://doi.org/10.21203/rs.3.rs-10929118/v1

License: This work is licensed under a Creative Commons Attribution 4.0 International License.
Read Full License

Additional Declarations: No competing interests reported.

Abstract

Integrative and conjugative elements carrying antimicrobial resistance genes have been reported in bovine mastitis-associated *Streptococcus uberis*. However, their broader distribution, structural characteristics, and transferability remain poorly understood. Analysis of 217 *S. uberis* genomes, including 37 newly sequenced Japanese mastitis isolates, identified ICE*tea*, a conserved integrative and conjugative element carrying *tet(O)*, *erm(B)*, and *aadE*, in 40% of Japanese isolates. ICE*tea* was approximately 66 kb, circularized, and integrated at the *rlmD* locus. Filter mating assays demonstrated transfer among *S. uberis* strains and from *S. uberis* to *Streptococcus agalactiae*, *Streptococcus pyogenes*, and *Staphylococcus aureus*, with antimicrobial-specific minimum inhibitory concentrations in transconjugants. ICE*tea*-like elements were detected in 6.0% of the human-derived *S. agalactiae* isolates examined and also identified in *Streptococcus ruminantium*, *Streptococcus suis*, and *Staphylococcus coagulans*. These findings establish ICE*tea* as a functionally validated, transferable multidrug-resistance element and support surveillance of mobile resistance elements across animal- and human-associated Gram-positive bacteria.

INTRODUCTION

Antimicrobial resistance (AMR) is a global health threat affecting human medicine, veterinary medicine, food production, and the environment[1]. Because humans, animals, and ecosystems are interconnected, AMR emergence and dissemination should be understood from a One Health perspective[2]. In food-producing animals, antimicrobials are essential for treating bacterial infections and maintaining animal welfare, but their use can impose selective pressure that promotes the persistence and spread of resistant bacteria and resistance genes[3]. Therefore, the monitoring of AMR in livestock-associated pathogens is important not only for animal health, but also for identifying resistance determinants with the potential to move across host and ecological boundaries.

Bovine mastitis is one of the most important infectious diseases in dairy cattle and remains a major driver of antimicrobial use on dairy farms[4]. Among mastitis-associated bacteria, *Streptococcus uberis* is a major environmental pathogen that causes clinical and subclinical intramammary infections in dairy cattle[5]. Bovine mastitis, including *S. uberis* mastitis, causes reduced milk production, increased somatic cell counts, treatment costs, and substantial economic losses[4,6]. Genomic studies have shown that *S. uberis* populations are highly diverse, with strain variation observed across regions and individual herds, consistent with its ecology as an environmental mastitis pathogen[5,7]. Antimicrobial agents are used in dairy herds to treat clinical mastitis during lactation and at drying-off, where blanket dry cow therapy has historically involved antimicrobial treatment, irrespective of infection status[4,8]. Repeated antimicrobial exposure during mastitis treatment and dry cow therapy may exert selective pressure on *S. uberis* populations circulating within dairy herds, potentially favoring resistant strains and mobile elements carrying resistance genes. These observations highlight the importance of understanding not only

antimicrobial resistance gene (ARG) carriage in *S. uberis*, but also the mobile genetic elements that mediate ARG persistence and dissemination[9,10].

Horizontal gene transfer is a major mechanism underlying the dissemination of AMR, with mobile genetic elements such as plasmids, transposons, and integrative and conjugative elements (ICEs) serving as important vehicles of resistance determinants[10,11]. ICEs are chromosomally integrated mobile genetic elements that can excise from the chromosome and transfer to recipient cells by conjugation. They typically encode functions required for integration, excision, and conjugative transfer, as well as accessory genes that may confer traits such as AMR[12]. Because ICEs can move between strains and, in some cases, between species, they may facilitate the dissemination of ARGs across bacterial populations associated with different hosts and ecological niches[12]. However, genome-based prediction alone does not demonstrate excision, circularization, or conjugative transfer; therefore, structural and functional validation is required to establish whether predicted ICEs represent complete and transferable elements[13]. Moreover, the physical linkage of multiple resistance genes on a single mobile element can lead to co-selection, whereby exposure to one antimicrobial class may maintain resistance genes against other antimicrobial classes encoded on the same element[10,14].

Despite accumulating evidence that *S. uberis* can harbor ARGs and ICE-associated resistance determinants, the epidemiological distribution, structural diversity, and functional transferability of such elements remain insufficiently resolved. Previous studies have shown that bovine streptococci, including *S. uberis*, can carry diverse ICEs associated with tetracycline, macrolide, and lincosamide resistance[15]. In Japan, AMR profiles of bovine milk-derived *S. uberis* isolates have recently been investigated, with *tet(O)*, *tet(S)*, *erm(B)*, *linB*, and *lnuD* linked to tetracycline, macrolide, and lincosamide resistance, and clonal complex 996 associated with multidrug resistance[9]. In addition, ICEs carrying *erm(B)* and *tet(O)* resistance determinants have been identified in antimicrobial-resistant *S. uberis* isolates from bovine milk in Chiba Prefecture, Japan[16]. However, the frequency and conservation of related ICEs among Japanese bovine mastitis-associated *S. uberis* isolates from different regions, their phylogenetic context within global *S. uberis* diversity, their experimentally validated transferability, and their occurrence in human- and other host-associated bacteria remain unclear.

Given this background, in the present study, we aimed to investigate ARG carriage and the associated mobile genetic elements in Japanese bovine mastitis-associated *S. uberis* from a One Health perspective. We first compared Japanese and global *S. uberis* genomes to define population structure and the distribution of resistance genes. We then identified and structurally characterized a conserved resistance-associated integrative and conjugative element, which we designated ICE*tea*, and determined its boundaries, attachment sites, and chromosomal integration site. Using filter mating assays, we tested the transferability of ICE*tea* to other Gram-positive species and evaluated its integration site and effects on antimicrobial susceptibility in transconjugants. Finally, to assess its broader relevance, we screened human-derived *Streptococcus agalactiae* and other Gram-positive taxa for ICE*tea*-like elements. This integrated approach combines structural and functional characterization of a multidrug-resistance

ICE with comparative genomic analysis of related elements across animal- and human-associated Gram-positive bacteria, providing a framework for mobile-element-level surveillance of AMR from a One Health perspective.

RESULTS

Identification of a conserved AMR-associated ICE in Japanese S. uberis isolates

We isolated and sequenced 37 *S. uberis* strains from milk samples of cows with mastitis in Hokkaido, Chiba, and Hiroshima, Japan. To examine population structure and ARG distribution, we analyzed 217 *S. uberis* genomes, comprising 37 newly sequenced Japanese isolates, 10 publicly available Japanese genomes, and 170 other publicly available genomes (47 Japanese genomes in total). Core-genome phylogeny showed geographic structuring, with most Japanese isolates forming a distinct cluster (Supplementary Fig. S1). For regional comparison, genomes were grouped into five geographic regions: Japan, Asia excluding Japan, Europe, Oceania, and the Americas.

ARGs were detected in 55% of Japanese isolates (26/47), compared with 86% of isolates from Asia excluding Japan (18/21), 42% from Europe (31/74), 29% from Oceania (14/49), and 0% from the Americas (0/26) (Supplementary Fig. S1). Among the 235 ARG detections, 51% were associated with macrolide–lincosamide–streptogramin resistance, 29% with aminoglycoside resistance, and 20% with tetracycline resistance. Among ARG-positive Japanese isolates, 76.9% carried the characteristic *erm(B)–aadE–tet(O)* gene pattern (Supplementary Fig. S2). Indicator analysis showed that *aadE* and *tet(O)* were strongly associated with Japanese isolates (indicator values 0.85 and 0.80, respectively), whereas *erm(B)* showed a moderate association (0.67) (Supplementary Table S1).

Next, we screened the 217 genomes for predicted ICEs using ICEscreen, a tool for detecting ICEs and integrative mobilizable elements (IMEs) in *Firmicutes*[13]. ICEscreen classifies ICE/IME-related elements based on the presence and organization of signature proteins, including relaxase, coupling protein, VirB4, and integrase. In total, 684 putative ICE/IME-related elements were detected, including 242 classified as “Complete ICE” by ICEscreen (Supplementary Table S2). Among these predicted complete ICEs, 32 carried ARGs. Notably, 19 Japanese *S. uberis* isolates harbored a predicted complete ICE carrying *tet(O)*, *erm(B)*, and *aadE* (19/47, 40%), which we designated ICE*tea*; the name *tea* was derived from these three resistance genes. The ICEscreen-predicted regions were 60,688–61,360 bp in length and highly conserved, and a BLASTn comparison using the ICE*tea* sequence from strain Hiro6 indicated that the other 18 elements showed 99%–100% query coverage and 99.9%–100% nucleotide identity. ICEscreen classified these elements as belonging to the Tn5252 family (Supplementary Table S3). In the analyzed *S. uberis* genome dataset, ICE*tea* was detected exclusively in Japanese isolates. Multilocus sequence typing analysis further showed that ICE*tea*-positive Japanese isolates were concentrated within specific sequence type groups (Fig. 1a).

Finally, we analyzed the antimicrobial susceptibility profiles of ICE*tea*-positive and ICE*tea*-negative isolates. Minimum inhibitory concentration (MIC) profiles for 14 antimicrobial agents were fitted as environmental vectors onto a principal coordinate analysis (PCoA) plot to identify the antimicrobial agents most strongly associated with variations in MIC profiles among the 37 newly sequenced Japanese isolates (Fig. 1b; Supplementary Table S4). Among the tested antimicrobial agents, lincomycin and erythromycin showed the strongest associations with the PCoA configuration (R^2 = 0.98 and R^2 = 0.95, respectively; both P = 0.001), followed by oxytetracycline (R^2 = 0.69, P = 0.001; Supplementary Table S5). Two-group comparisons of MIC values between ICE*tea*-positive and ICE*tea*-negative isolates revealed significant differences for all three agents after false discovery rate (FDR) correction (Fig. 1c; Supplementary Table S5). Significant differences were also observed for several β-lactams (ampicillin, amoxicillin, cefazolin, and penicillin G; FDR-adjusted $P < 0.05$; Supplementary Table S5). However, all isolates remained susceptible to these agents (resistance rate 0%; Supplementary Table S4), and ICE*tea* carried no β-lactam resistance determinant. No significant difference was observed for gentamicin (FDR-adjusted P = 1.000). Together, these results identify ICE*tea* as a conserved AMR-associated ICE carrying *tet(O)*, *erm(B)*, and *aadE* in Japanese bovine mastitis-associated *S. uberis* and indicate that its carriage is associated with specific sequence type groups and differences in antimicrobial susceptibility profiles.

Structural characterization and chromosomal integration of ICE tea

Because ICEscreen does not define exact element boundaries, we determined the ICE*tea* termini by PCR amplification and sequencing of its circular junction in 10 ICE*tea*-positive *S. uberis* strains (Supplementary Fig. S3). The integrated ICE*tea* elements were 66,280–66,281 bp and nearly identical among the 10 strains (Supplementary Table S3). Annotation of the 66,281-bp ICE*tea* sequence from strain Hiro6 predicted 63 genes. In addition to resistance genes, ICE*tea* carried several genes associated with lantibiotic biosynthesis, regulation, transport, and immunity (CDS_54–CDS_61) and three toxin–antitoxin systems: epsilon–zeta, PezA–PezT, and AbiEi–AbiEii (Fig. 2a; Supplementary Table S6). Analysis of the integration site showed that the core sequence of *attL*, *attR*, *attP*, and *attB* was 5'-CACGT-3' (Fig. 2b). In all examined strains, ICE*tea* was integrated at the 3' end of the *rlmD* gene, which encodes a 23S rRNA methyltransferase. The conserved attachment-site core sequence was consistent with site-specific recombination at this locus.

Experimental transfer of ICE tea from S. uberis to recipient bacteria

We examined the transferability of ICE*tea* from *S. uberis* using filter mating assays. First, transfer among *S. uberis* strains was tested using five ICE*tea*-positive donors—Hiro6, ZQ9, ZQ22, ZQ-y1, and ZQ-y4—and one recipient strain, ZQ1. ICE*tea* transfer was detected in all these donor–recipient combinations, with transfer efficiencies ranging from 10^{-7} to 10^{-5} transconjugants per recipient (Fig. 3a; Supplementary Table S7). Overall, transfer efficiencies differed among donor–recipient combinations (Kruskal–Wallis test, H = 13.11, $P < 0.0001$), although no individual pairwise comparison was significant in Dunn's multiple comparisons test.

To assess interspecies transfer of ICE*tea*, we used ICE*tea*-positive *S. uberis* Hiro6 as the donor, and *S. uberis* ZQ12, vaginal-swab-derived *S. agalactiae* strains GBS3 and GBS5, patient-derived *Streptococcus pyogenes* strains GAS5001 and GAS5006, *Staphylococcus aureus* RN4220, and *Escherichia coli* DH5α as recipients. ICE*tea* transferred to *S. uberis*, *S. agalactiae*, *S. pyogenes*, and *S. aureus*, but not to *E. coli*. Transfer efficiencies ranged from 10^{-9} to 10^{-7} transconjugants per recipient for streptococcal recipients and approximately 10^{-11} for *S. aureus* (mean of at least three independent experiments; Fig. 3b; Supplementary Table S7). Transfer efficiencies differed significantly among recipient strains (Kruskal–Wallis test, $H = 20.13$, $P = 0.0026$). Dunn's multiple comparisons test showed significant differences between GBS3 and RN4220 (adjusted $P = 0.0308$) and between GBS3 and DH5α (adjusted $P = 0.0141$); no other pairwise comparisons were significant.

Genome analysis of transconjugants confirmed acquisition of ICE*tea* without detectable major rearrangements in the ICE*tea* backbone. Comparison of parental recipient *attB* sequences with transconjugant junctions confirmed the expected *attL* and *attR* attachment-site motifs (Supplementary Table S8). In some transconjugants, when the central base of the recipient *attB* core sequence was T rather than C, the *attL* sequence remained unchanged, whereas the corresponding central base in *attR* was T (Supplementary Table S8). In all recipient species from which transconjugants were obtained, including *S. aureus*, ICE*tea* integrated into the *rlmD* locus, consistent with the integration site identified in the original *S. uberis* isolates. The *rlmD* coding sequence remained uninterrupted following ICE*tea* integration in all examined transconjugants; the encoded RlmD proteins (i.e., 23S rRNA methyltransferases) differed by only 1–8 amino acids among recipient strains. Together, these results demonstrate that ICE*tea* integrates at the *rlmD* locus in multiple Gram-positive recipient taxa.

Next, we compared antimicrobial susceptibility profiles between parental recipient strains and their corresponding ICE*tea*-carrying transconjugants. MICs of erythromycin and lincomycin were significantly increased following ICE*tea* acquisition after adjustment for multiple comparisons (adjusted $P = 0.0391$ for both). Tetracycline MICs increased in six of seven independent recipient backgrounds and streptomycin MICs in five of seven, although these changes did not reach statistical significance after adjustment for multiple comparisons (adjusted $P = 0.0521$ and 0.0781, respectively) (Supplementary Table S9). Overall, the observed MIC changes following ICE*tea* acquisition were consistent with the resistance determinants carried by the element, including *erm(B)*, *tet(O)*, and *aadE*, although statistically significant increases after multiple-comparison adjustment were observed only for erythromycin and lincomycin.

ICE tea -like elements in human-derived S. agalactiae isolates from Japan

To examine whether ICE*tea*-like elements are present in human-associated *S. agalactiae* in Japan, we screened 67 isolates, comprising 36 vaginal-swab isolates from women and 31 blood isolates from patients, using PCR targeting the ICE*tea* circular junction, integrase, *tet(O)*, *erm(B)*, and *aadE*. In this screening, isolates positive for both the ICE*tea* circular junction and integrase were considered presumptively positive for an ICE*tea*-like element. Four isolates—GBS26, GBS128, GBS184, and

OUGBS105—met this criterion. The *tet(O)* and *erm(B)* genes were detected in all four isolates, whereas *aadE* was detected in GBS26 and GBS184 (Supplementary Table S10). When the four isolate genomes were subsequently analyzed using ICEscreen, all four were predicted to carry a single ICE*tea*-like element classified as “Complete ICE.” ICE*tea*-like elements were detected in 6.0% (4/67) of human-derived *S. agalactiae* isolates: 8.3% (3/36) of vaginal-swab isolates and 3.2% (1/31) of blood isolates. Comparative analysis of the gene structures of the four ICE*tea*-like elements revealed insertions and partial deletions when compared with ICE*tea* identified in *S. uberis* (Fig. 4a). In particular, the inserted regions primarily contained ARGs and transposase genes.

Environmental vector fitting of the MIC-based PCoA identified erythromycin, azithromycin, the erythromycin/clindamycin combination, clarithromycin, and minocycline as the antimicrobial agents most strongly associated with variation in the ordination (R^2 = 0.92, 0.90, 0.80, 0.79, and 0.76, respectively; P = 0.001 for all), followed by clindamycin (R^2 = 0.59, P = 0.001; Fig. 4b; Supplementary Tables S11 and S12). After FDR correction, MICs differed significantly between ICE*tea*-like element-positive and -negative isolates for erythromycin, azithromycin, the erythromycin/clindamycin combination, clarithromycin, and clindamycin, but not minocycline (Fig. 4c; Supplementary Table S12).

Finally, we examined the transferability of ICE*tea*-like elements from four *S. agalactiae* isolates—GBS26, GBS128, GBS184, and OUGBS105—by filter mating assays using *S. agalactiae* GBS3 and GBS5 and *S. uberis* ZQ1 and ZQ12 as recipients (Supplementary Table S13). Transfer of ICE*tea*-like elements was detected in five donor–recipient combinations involving GBS128, GBS184, and OUGBS105, with transfer efficiencies ranging from 10^{-9} to 10^{-5}, whereas no transfer was detected from GBS26.

Distribution and comparative analysis of ICE tea -like elements across Gram-positive bacterial taxa

To assess the broader distribution of ICE*tea*-like elements, we screened 1,079 genomes, comprising 1,042 publicly available RefSeq genomes and the 37 *S. uberis* genomes sequenced in this study. The four *S. agalactiae* genomes sequenced after PCR-positive selection were excluded from proportion calculations but retained for subsequent phylogenetic and structural analyses. ICE*tea*-like elements were defined as genomic regions showing ≥ 80% query coverage and ≥ 95% nucleotide identity to the ICE*tea* sequence of *S. uberis* Hiro6 by BLASTn. The detected regions were subsequently classified by ICEscreen as “Complete ICE” or “Other” (see Methods). ICE*tea*-like elements were detected in *S. uberis*, *Streptococcus ruminantium*, *S. agalactiae*, *Streptococcus suis*, and *Staphylococcus coagulans*, but not in the analyzed *S. pyogenes* genomes (Fig. 5; Supplementary Fig. S4). We then compared the proportions of genomes carrying ICE*tea*-like elements and their ICEscreen-predicted completeness across bacterial species and host origins. Although no ICE*tea*-like elements were detected in the non-Japanese *S. uberis* genomes analyzed, ICE*tea* was identified in 40% of Japanese bovine mastitis-associated isolates, and all detected elements were classified as “Complete ICE.” In *S. ruminantium*, ICE*tea*-like elements were detected in 38% of the analyzed genomes, all of which were derived from Japan, with most being classified as “Complete ICE.” In *S. suis*, ICE*tea*-like elements were detected in both human- and pig-derived genomes, in 31% and 8% of the analyzed genomes, respectively, and all detected elements were

classified as “Complete ICE.” In *S. agalactiae*, ICE*tea*-like elements were detected in 17%, 5%, and 2% of the analyzed human-, cattle-, and other host-derived genomes, respectively, and all detected elements were classified as “Complete ICE.” In *S. coagulans*, ICE*tea*-like elements were detected in 21% of the analyzed genomes and classified as “Other” rather than “Complete ICE” by ICEscreen (Fig. 5; Supplementary Fig. S4).

For subsequent phylogenetic analysis, we combined the ICE*tea*-like elements identified in the 1,079-genome screening dataset with the four ICE*tea*-like elements from the *S. agalactiae* isolates sequenced after PCR-positive selection. Highly similar sequences were clustered to reduce redundancy, and representative elements were selected from each cluster. The final dataset comprised 44 representative ICE*tea*-like elements, including all four elements from the *S. agalactiae* isolates sequenced in this study. Maximum-likelihood phylogenetic analysis based on seven conserved genes associated with ICE conjugation and maintenance showed that ICE*tea*-like elements from different bacterial species were interspersed across the tree, with no clear clustering according to bacterial species, host origin, or geographic region (Fig. 6a). ICE*tea* from *S. uberis* was most closely related to ICE*tea*-like elements from human-associated *S. agalactiae* and cattle-derived *S. ruminantium*, followed by elements from dog-derived *S. coagulans* and human-and-pig-derived *S. suis*. Among the *S. agalactiae* elements, those identified in this study, including ICE*tea*-like elements from vaginal swab-derived *S. agalactiae* strains GBS26 and GBS184, were positioned relatively close to *S. uberis* ICE*tea*.

We then compared the genetic organization of representative ICE*tea*-like elements from different bacterial species. ICE*tea* in *S. uberis* and ICE*tea*-like elements in *S. ruminantium* shared highly conserved backbone structures (Fig. 6b). By contrast, ICE*tea*-like elements from *S. agalactiae* and *S. suis* contained additional accessory regions, including ARGs and transposase-related genes. These results indicate that ICE*tea*-like elements occur across multiple Gram-positive bacterial taxa and share a conserved ICE-associated backbone while differing in accessory gene content.

DISCUSSION

This study identified ICE*tea* as a highly conserved and transferable multidrug-resistance ICE in Japanese bovine mastitis-associated *S. uberis*. ICE*tea* carries *tet(O)*, *erm(B)*, and *aadE*, is associated with differences in antimicrobial susceptibility, and transfers experimentally to multiple Gram-positive species. Together, structural characterization and filter mating assays establish ICE*tea* as a functional multidrug-resistance ICE capable of interspecies transfer among Gram-positive bacteria under laboratory conditions.

The high proportion of ICE*tea*-positive isolates among the Japanese *S. uberis* analyzed in the present study raises the question of how this element is maintained in this population. Its detection in 40% of Japanese isolates, but not in the non-Japanese genomes examined, suggests a geographically skewed distribution within the available dataset. This pattern may reflect clonal expansion of ICE*tea*-positive lineages, horizontal transfer among cattle-associated streptococci, antimicrobial selection in Japanese

dairy systems, or a combination of these processes[9,15,17,18]. Genes carried by ICE*tea* may also contribute to its maintenance. *S. uberis* can produce lantibiotics and other bacteriocin-like inhibitory substances[19], and ICE*tea* carries several genes associated with lantibiotic biosynthesis, regulation, transport, and immunity (Fig. 2a; Supplementary Table S6), which may contribute to lantibiotic production or immunity. ICE*tea* also encodes PezA/PezT, epsilon–zeta, and AbiE toxin–antitoxin systems. Homologous type II and type IV toxin–antitoxin systems were recently shown to stabilize a multidrug-resistance ICE in *S. suis*[20], suggesting that these systems may similarly promote ICE*tea* maintenance. These proposed functions remain to be experimentally validated.

The antimicrobial stewardship relevance of ICE*tea* lies primarily in the potential for co-selection of linked resistance determinants rather than in direct compromise of β-lactam therapy. Because ICE*tea* physically links *tet(O)*, *erm(B)*, and *aadE*, exposure to one corresponding antimicrobial class may favor maintenance of the entire element and thereby co-select resistance to the others[10,14]. This may be particularly relevant in Japan, where tetracyclines account for a large proportion of veterinary antimicrobial use in food-producing animals[17], and dihydrostreptomycin is among the antimicrobials commonly administered by the intramammary route on Japanese dairy farms[18]. By contrast, although MICs for several β-lactams differed between ICE*tea*-positive and ICE*tea*-negative isolates, all isolates remained susceptible, and ICE*tea* carries no known β-lactam resistance determinant. Thus, these differences should not be interpreted as an ICE*tea*-mediated β-lactam resistance phenotype. The principal stewardship implication is that exposure to tetracyclines, macrolides/lincosamides, or streptomycin/dihydrostreptomycin may favor maintenance of the entire multidrug-resistance element even when selection acts on only one resistance determinant. These findings reinforce the rationale for minimizing unnecessary antimicrobial exposure through mastitis prevention, culture- or susceptibility-guided therapy where feasible, and selective rather than blanket dry cow therapy[8,21].

Previous studies have identified diverse resistance-associated ICEs in bovine *S. agalactiae*, *Streptococcus dysgalactiae* subsp. *dysgalactiae*, and *S. uberis*[15], while Tn916/Tn1545-family elements represent well-characterized conjugative resistance elements in Gram-positive bacteria[22]. ICEs carrying *erm(B)* and *tet(O)* have also recently been reported in bovine *S. uberis* in Japan[16]. The present study extends these observations by demonstrating ICE*tea* circularization, defining its attachment sites and *rlmD* integration, and experimentally linking ICE*tea* acquisition to antimicrobial-specific changes in MICs consistent with its encoded resistance determinants.

A central remaining question is whether ICE*tea*-like elements can cross the animal–human interface and, if so, whether the direction of such exchange can be inferred. Previous studies have documented AMR exchange across this interface, although directionality cannot be inferred from host origin alone[23,24], and host transitions between bovine and human populations have been reported in *S. agalactiae*[25]. In the present study, circularization, conjugative transfer, *rlmD*-specific integration, and acquisition-associated changes in antimicrobial susceptibility established conjugation as a functional mechanism of ICE*tea* transfer. ICE*tea* therefore represents an experimentally validated conjugative route for ARG transfer. Its

experimental recipient range extended beyond its observed genomic distribution: ICE*tea* transferred from *S. uberis* to *S. agalactiae*, *S. pyogenes*, and *S. aureus*, despite the absence of ICE*tea*-like elements in the analyzed *S. pyogenes* genomes. Transfer to *S. aureus* is noteworthy given the importance of mobile genetic elements in resistance and virulence dissemination in this species[26], although it does not establish *S. aureus* as a natural reservoir of ICE*tea*. Importantly, conjugative transfer of ICE*tea* or ICE*tea*-like elements between *S. uberis* and *S. agalactiae* was observed in both directions under laboratory conditions (Supplementary Tables S7 and S13). In our experimental system, *S. uberis*-derived ICE*tea* transferred to both tested *S. agalactiae* recipients, whereas transfer of *S. agalactiae* ICE*tea*-like elements to *S. uberis* was donor- and recipient-dependent. Although this pattern may reflect differences in host compatibility, the limited number of strains and the different donor–recipient combinations preclude firm conclusions regarding directional bias. At the genomic level, ICE*tea* was highly conserved among Japanese bovine mastitis-associated *S. uberis*, whereas ICE*tea*-like elements in human-derived *S. agalactiae* were structurally more heterogeneous. The *S. agalactiae* population itself was also genetically diverse and lacked the clear geographic clustering observed in *S. uberis* (Supplementary Fig. S5), consistent with the occurrence of ICE*tea*-like elements across multiple genetic backgrounds. Together, these findings are compatible with, but do not demonstrate, cross-host exchange of ICE*tea*-like elements between animal- and human-associated streptococci and with their occurrence across diverse genetic backgrounds. However, the present data do not resolve the direction of such exchange, and direct animal-to-human transmission cannot be established; bidirectional exchange, intermediate hosts, and shared reservoirs remain possible.

The clinical significance of ICE*tea*-like elements in human-associated *S. agalactiae* remains uncertain. Penicillin remains the first-line agent for intrapartum GBS prophylaxis, whereas clindamycin is recommended only for selected patients with high-risk β-lactam allergy when the isolate is confirmed to be susceptible[27]. Because macrolide and clindamycin resistance in *S. agalactiae* is frequently mediated by *erm* genes[28], carriage of *erm(B)*-containing ICE*tea*-like elements may be clinically relevant, particularly when clindamycin is used for intrapartum prophylaxis in patients with high-risk β-lactam allergy. However, among our isolates, ICE*tea*-like element carriage was associated with only a subset of the observed differences in antimicrobial susceptibility. Larger clinical datasets linking mobile-element structure with antimicrobial exposure and clinical outcomes are therefore required to establish their clinical significance.

Plasmids are widely recognized as major vehicles of horizontal ARG transfer[10]. However, chromosomally integrated mobile elements such as ICEs represent another important route for the maintenance and dissemination of resistance determinants[12]. Because ICEs can persist within the bacterial chromosome while retaining the capacity for excision and conjugative transfer, they combine stable vertical inheritance with the potential for horizontal spread[12]. In the present study, the occurrence of closely related ICE*tea*-like elements across multiple Gram-positive taxa and host origins, together with the experimentally demonstrated interspecies transfer of ICE*tea*, supports consideration of ICEs alongside plasmids in One Health AMR surveillance[24]. Surveillance strategies that track mobile genetic elements

themselves, in addition to bacterial lineages and individual ARGs, may provide a more complete view of multidrug-resistance dissemination across animal- and human-associated bacterial populations.

This study has several limitations. Public genome datasets are affected by geographic and temporal sampling gaps, uneven host metadata, species-specific sampling intensity, and variable assembly quality, which may influence the apparent frequency and host distribution of mobile genetic elements[24,29]. Accordingly, comparative genomic relatedness alone cannot establish transmission directionality[23,29]. Farm-level antimicrobial use, treatment histories, and clinical outcomes were unavailable, and filter mating measures transfer potential under laboratory conditions rather than in vivo transfer frequency. In addition, computational prediction does not establish ICE functionality[13]: GBS26 was classified as a "Complete ICE," but no transfer was detected under our assay conditions, which may reflect structural differences from *S. uberis* ICE*tea* (Fig. 4a), the specific mating conditions used, or other donor–recipient compatibility factors. Future studies integrating longitudinal sampling across animals, humans, and the environment with long-read sequencing, antimicrobial-use data, and functional assays are required to resolve the epidemiology and direction of ICE*tea*-like element movement.

In conclusion, ICE*tea* represents a conserved and experimentally validated multidrug-resistance ICE in bovine mastitis-associated *S. uberis*. Its ability to transfer between Gram-positive species, together with the occurrence of related elements in bacteria from animal and human hosts, highlights the potential role of transferable mobile elements in AMR dissemination across ecological and host boundaries. Although no direct animal-to-human transmission was demonstrated, the present findings provide a basis for tracing the distribution, diversification, and movement of ICE*tea*-like elements within a One Health framework.

METHODS

Bacteria, culture media, and culture conditions

The *S. uberis* strains were isolated by veterinarians from milk collected from cows with mastitis in Japan. The *S. agalactiae* strains comprised vaginal-swab isolates obtained in our previous study[30] and clinical isolates provided by the Clinical Microbiology Laboratory of Okayama University Hospital. All bacterial strains were stored at − 80 °C until use. *Streptococcus* spp. were cultured microaerobically at 37 °C in Todd–Hewitt medium (Becton, Dickinson and Co., Franklin Lakes, NJ, USA), whereas *S. aureus* and *E. coli* were cultured aerobically at 37 °C in Luria–Bertani (LB) medium (Kanto Chemical Co., Tokyo, Japan), unless otherwise stated.

Genomic DNA extraction and sequencing

Genomic DNA was obtained from bacteria using an ISOSPIN Fecal DNA kit (Nippon Gene Co., Tokyo, Japan), according to the manufacturer's instructions.

Short-read whole-genome sequencing was outsourced to Genome-Lead Co., Ltd. (Kagawa, Japan). Two short-read sequencing platforms were used, with the platform and read configuration for each isolate provided in Supplementary Table S14. First, library preparation was performed using the Illumina DNA Prep Tagmentation Kit (Illumina, San Diego, CA, USA) according to the manufacturer's instructions, and sequencing was conducted on a NextSeq 1000 system using NextSeq 1000/2000 P2 300M reagents (600 cycles; Illumina). Second, libraries were constructed using the MGIEasy Fast FS Library Prep Set (MGI Tech, Shenzhen, China), and 2 · 150 bp paired-end sequencing was performed on a DNBSEQ-G400RS sequencer using a DNBSEQ-G400 High-throughput Sequencing Set (MGI Tech).

For gap closure, target gap regions were amplified by PCR when necessary using PrimeSTAR Max DNA Polymerase Ver.2 (Takara Bio, Shiga, Japan). The resulting PCR products were subjected to Oxford Nanopore long-read sequencing through the PCR-EZ service provided by GENEWIZ (Azenta Japan Corp., Tokyo, Japan).

Short sequencing reads were trimmed using fastp v0.23.4[31] and assembled using SPAdes v4.2.0[32]. Oxford Nanopore reads generated from PCR-amplified gap regions were combined with the short-read data in SPAdes v4.2.0 to resolve the corresponding gaps. Genome assembly statistics, including genome size, number of contigs, N50, and G + C content, were calculated using QUAST v5.2.0 with the default minimum contig length of 500 bp[33]. Details of all newly sequenced genomes are provided in Supplementary Table S14.

Genome sequences used for comparison

Bacterial genomes were downloaded from the NCBI RefSeq database using ncbi-genome-download v0.3.3[34]. The public dataset comprised 180 *S. uberis* genomes (accessed on 11 June 2025) and 206 *S. agalactiae*, 411 *S. pyogenes*, 197 *S. suis*, 24 *S. ruminantium*, and 24 *S. coagulans* genomes (accessed on 1 April 2026), yielding 1,042 publicly available genomes. Together with the 37 *S. uberis* genomes newly sequenced in this study, 1,079 genomes were included in comparative proportion analyses. The four *S. agalactiae* genomes sequenced after PCR-positive selection were excluded from proportion calculations, but included in subsequent phylogenetic and structural analyses. Accession numbers and metadata are provided in Supplementary Table S15.

Genome analysis

All genomes were annotated using Prokka v1.14.6[35]. Core-genome analyses were performed separately for *S. uberis* and *S. agalactiae*. Core genes were identified using Roary v3.13.0[36] with a 95% BLASTp identity threshold, and concatenated core-gene alignments were generated using MAFFT implemented in Roary[36,37]. Phylogenetic trees were inferred from the concatenated core-gene nucleotide alignments using FastTree v2.2.0 under the GTR + CAT model (-gtr -nt)[38] and visualized using Interactive Tree of Life (iTOL) v7[39]. ARGs were detected by AMRFinderPlus v4.0.19[40] with thresholds of ≥ 80% coverage and ≥

90% identity. A heatmap was visualized using the pheatmap package v1.0.13 in R v4.5.1[41,42]. Indicator analysis of ARG occurrence across geographic regions was performed using the indicspecies package v1.8.0[43] in R v4.5.1, with significance assessed using 999 permutations. Indicator values were categorized as strong (> 0.70), moderate (0.50–0.70), weak-to-moderate (0.30–0.50), or weak (< 0.30). Sequence types (STs) were assigned using mlst v2.23.0[44] and the *S. uberis* PubMLST scheme[45]. PHYLOViZ v2.0[46] with the goeBURST Full MST algorithm was used to construct a minimum spanning tree, which was color-coded by geographic regions. ICEs were predicted using ICEscreen v1.3.3[13].

Antimicrobial susceptibility testing and MIC-based analyses

The MICs of antimicrobial agents were determined by broth microdilution. For *S. uberis*, resistance was interpreted using CLSI VET01S criteria where applicable[47]; for antimicrobial agents lacking applicable CLSI criteria, previously published interpretive criteria were used[48,49]. For human-derived *S. agalactiae*, resistance was interpreted according to CLSI M100[50], as detailed in Supplementary Table S11.

Cation-adjusted Mueller–Hinton broth (Becton, Dickinson and Co.) was used for staphylococci, whereas cation-adjusted Mueller–Hinton broth (Becton, Dickinson and Co.) supplemented with 3% lysed horse blood (Nippon Bio-Supp. Center, Tokyo, Japan) was used for streptococci. MICs were defined as the lowest concentrations that completely inhibited visible bacterial growth. For human-derived *S. agalactiae* isolates, antimicrobial susceptibility testing was performed using Dry Plate 'Eiken' DP44 (Eiken Chemical, Tokyo, Japan). The antimicrobial agents tested are listed in Supplementary Table S16.

For MIC-based PCoA and Mann–Whitney *U* analyses, off-scale MIC values were assigned to the next twofold dilution beyond the tested range; for example, values > 64 μg/mL were assigned as 128 μg/mL and values < 1 μg/mL as 0.5 μg/mL. MIC values were then $\log_2$-transformed before multivariate analysis. PCoA based on Euclidean distances calculated from the $\log_2$-transformed MIC values was conducted in R v4.5.1 using the ape package (v5.8-1)[51], and environmental vector fitting (envfit) with 999 permutations was performed using vegan v2.7-5[52] to identify the variables most strongly associated with the ordination. MIC values of individual antimicrobial agents were compared between ICE*tea*-positive and -negative *S. uberis* isolates and between ICE*tea*-like element-positive and -negative *S. agalactiae* isolates using two-sided Mann–Whitney *U* tests. *P*-values from the two-group MIC comparisons were adjusted for multiple comparisons using the Benjamini–Hochberg FDR method (p.adjust function) in R v4.5.1. FDR-adjusted *P*-values < 0.05 were considered statistically significant. Data visualization was performed using ggplot2 v3.5.2 in R v4.5.1[41].

PCR amplification and sequencing

PCR was conducted using FastGene 2· PCR Master Mix (Nihon Genetics Co., Tokyo, Japan). Heat-treated bacterial cell suspensions (95 °C for 10 minutes) were used as PCR templates. Primer sequences,

expected product sizes, and PCR cycling conditions are provided in Supplementary Table S17.

For ICE*tea* boundary determination, PCR was performed on 10 ICE*tea*-positive *S. uberis* strains using five primer sets designed to amplify the junction region of the circularized element and its terminal regions (Supplementary Fig. S3; Supplementary Table S17). The circular-junction amplicon was subjected to Sanger sequencing and compared with the corresponding chromosomal regions to define the boundaries of the integrated ICE*tea* element. Sanger sequencing was outsourced to GENEWIZ (Azenta Japan Corp.).

To screen human-derived *S. agalactiae* for ICE*tea*-like elements, PCR assays targeting the ICE*tea* circular junction, integrase, *tet(O)*, *erm(B)*, and *aadE* were performed. Isolates positive for both the circular junction and integrase were considered presumptively positive for an ICE*tea*-like element and subsequently subjected to whole-genome sequencing and ICEscreen analysis.

Filter mating assay

Rifampicin- and fusidic acid-resistant derivatives of streptococcal recipient strains were generated by stepwise exposure to increasing concentrations of rifampicin and fusidic acid, with final selection concentrations of 25 and 10 μg/mL, respectively. Donor and recipient strains used in conjugation experiments are listed in Supplementary Tables S7 and S13.

Filter mating assays were performed as previously described, with minor modifications[15,53]. Donor and recipient strains were cultured separately to mid-log phase, adjusted to approximately $5 \cdot 10^8$ colony-forming units (CFUs)/mL, mixed in equal volumes, and collected onto 25-mm-diameter, 0.2-μm-pore-size filter membranes (ADVANTEC, Tokyo, Japan). The filters were placed on Todd–Hewitt agar (Becton, Dickinson and Co.) and incubated at 37 °C for 18 h. Bacteria were then recovered from the filters in 1 mL of PBS, serially diluted, and plated on selective media. Transconjugants of *S. uberis*, *S. agalactiae*, and *S. pyogenes* were selected on media containing rifampicin (25 μg/mL), fusidic acid (10 μg/mL), and erythromycin (10 μg/mL). *S. aureus* transconjugants were selected on LB agar (Kanto Chemical Co.) supplemented with 7.5% NaCl and erythromycin (10 μg/mL), and *E. coli* transconjugants were selected on deoxycholate-hydrogen sulfide-lactose agar (Shimadzu Diagnostics Corp., Tokyo, Japan) supplemented with tetracycline (5 μg/mL) and streptomycin (50 μg/mL).

Transfer efficiency was calculated as the number of transconjugant CFUs divided by the number of recipient CFUs recovered on recipient-selective media. Transfer efficiencies were determined from at least three independent experiments. To enable $\log_{10}$ transformation of zero values, a pseudocount of $1 \cdot 10^{-13}$ was added to all transfer-efficiency values before $\log_{10}$ transformation. The transformed values were analyzed using the Kruskal–Wallis test followed by Dunn's multiple comparisons test in GraphPad Prism v8.0.2 (GraphPad Software Inc., San Diego, CA, USA). *P*-values < 0.05 were considered statistically significant for the overall Kruskal–Wallis test, and Dunn-adjusted *P*-values < 0.05 were considered statistically significant for pairwise comparisons.

Changes in MIC between parental recipient strains and corresponding ICE*tea*-carrying transconjugants were analyzed for each antimicrobial agent using a two-sided exact sign test implemented with the binom.test function in R v4.5.1[41]. Each independent recipient background was treated as one paired observation; multiple transconjugants derived from the same recipient background were treated as a single observation. Ties were excluded. *P*-values were adjusted for multiple comparisons using the Benjamini–Hochberg method (p.adjust, method = "BH") in R v4.5.1[41], with adjusted *P*-values < 0.05 considered statistically significant.

Whole-genome sequences of transconjugants were assembled as described above. The chromosomal insertion site of ICE*tea* was identified by BLASTn v2.12.0 + [54] searches of the assembled genomes, and the flanking sequences were examined to confirm integration at the *rlmD* locus and corresponding attachment-site sequences. The assembled ICE*tea* regions were compared with donor ICE*tea* by BLASTn to assess large-scale structural differences. The *rlmD* coding sequences and deduced RlmD amino acid sequences were also compared among parental recipient strains and corresponding transconjugants.

Screening, phylogenetic analysis and sequence comparison of ICE tea -like elements

For comparative distribution analysis, the 1,079-genome dataset described above was screened for ICE*tea*-like elements using BLASTn v2.12.0 + [54], with the ICE*tea* sequence from *S. uberis* Hiro6 as the query. The four *S. agalactiae* genomes sequenced after PCR-positive selection were screened using the same criteria and included only in subsequent phylogenetic and structural analyses. Candidate regions were defined using thresholds of ≥ 80% query coverage and ≥ 95% nucleotide identity. Candidate ICE*tea*-like regions were then extracted and classified using ICEscreen v1.3.3[13].

For phylogenetic analysis, ICE*tea*-like elements identified in the 1,079-genome screening dataset were combined with the four ICE*tea*-like elements from the *S. agalactiae* isolates sequenced after PCR-positive selection. Representative sequences were then selected from this combined dataset. Mash distance, a *k*-mer-based estimate of sequence distance between two DNA sequences, was calculated using Mashtree v1.2.0[55]. Based on the Mash distance matrix, highly similar sequences (Mash distance < 0.0001) were clustered using complete-linkage hierarchical clustering with the hclust function in R v4.5.1[41]. A representative sequence was selected from each cluster as the sequence with the lowest mean pairwise Mash distance to all other sequences within the same cluster. This selection was implemented using the dplyr package v1.2.1 in R[56].

We then conducted phylogenetic analysis using the representative ICE*tea*-like sequences. Sequences were annotated using Prokka v1.14.6, and conserved domains were identified using the NCBI conserved domain database[57]. Nucleotide sequences of the orthologous genes were extracted and aligned independently using MAFFT v7[37]. Seven conserved genes associated with ICE conjugation or maintenance were selected from the ICE*tea*-like backbone of all representative elements for phylogenetic analysis: relaxase, VirD4, VirB4, MobC, Tn5252_Orf10, TnpV, and PrgI. When additional homologs were present within nested ICE regions, these were excluded, and only the ortholog

corresponding to the ICE*tea*-like backbone was retained. The individual gene alignments were concatenated into a partitioned alignment using AMAS v1.0[58], with gene boundaries retained as separate partitions. Maximum-likelihood phylogenetic analysis was performed using IQ-TREE v3.1.2[59]. The optimal partitioning scheme and nucleotide substitution models were selected using ModelFinder with partition merging (-m MFP+MERGE). Branch support was assessed using 1,000 ultrafast bootstrap replicates and 1,000 SH-aLRT replicates. The resulting tree was visualized using Interactive Tree of Life (iTOL) v7. Comparative visualization of ICE sequences was performed using Easyfig v2.2.5[60].

Declarations

ETHICS STATEMENT

This study used only bacterial isolates and did not involve the collection of human or animal samples specifically for research purposes, or the collection of additional clinical data or personal information.

The *S. uberis* isolates were obtained from milk samples collected by veterinarians as part of the routine clinical diagnosis of bovine mastitis, and no animals were sampled specifically for this study. Accordingly, no additional animal ethics review or approval was required under the relevant regulations of Okayama University.

The vaginal-swab-derived *S. agalactiae* isolates were obtained in our previous study[30], which was approved by the Kitasato Institute Hospital Research Ethics Committee (approval No.: 19060). The requirement for informed consent was waived by the Ethics Committee. The clinical *S. agalactiae* isolates were provided by the Clinical Microbiology Laboratory of Okayama University Hospital as anonymized bacterial isolates without accompanying personal or clinical information and could not be linked to individual patients. Accordingly, under the Ethical Guidelines for Medical and Biological Research Involving Human Subjects (Ministry of Education, Culture, Sports, Science and Technology; Ministry of Health, Labour and Welfare; and Ministry of Economy, Trade and Industry, Japan) and the relevant regulations of Okayama University, the use of these anonymized bacterial isolates did not require additional ethics review or approval.

COMPETING INTERESTS

SO and TT are employees of Nippon Zenyaku Kogyo Co., Ltd. The company had no role in the study design, data analysis, interpretation of the results, or decision to submit the manuscript for publication. The authors declare no other competing interests.

Author Contribution

J.U. and H.Ma. conceived and designed the study. T.W., H.Ma., J.U., P.M., and I.U. performed the experiments. J.U., T.Y., N.S., S.O., T.T., and H.Mu. contributed strains, resources, and data. T.W. and J.U. analyzed the data and wrote the manuscript. H.Ha. and J.U. supervised the study. All authors reviewed and approved the final version of the manuscript.

Acknowledgement

We thank the Clinical Microbiology Laboratory of Okayama University Hospital for providing the clinical S. agalactiae isolates used in this study. This work was supported by the Small-Business Innovation Research (SBIR) Program of the Bio-oriented Technology Research Advancement Institution (BRAIN), Japan (grant no. SU24A03). The funder had no role in study design, data collection and analysis, interpretation of the results, or the decision to submit the manuscript for publication.

Data Availability

The genome sequences generated in this study have been deposited in GenBank/DDBJ under BioProject accessionsaccession numbers PRJDB35858, PRJDB42709, and PRJDB42710. Individual assembly accession numbers are provided in Supplementary Table S14. Accession numbers and metadata for all genomes used in the comparative analyses are provided in Supplementary Table S15.

CODE AVAILABILITY

No custom software or algorithms were developed for this study. All analyses were performed using publicly available software packages described in the Methods with the parameters specified therein. R scripts used for statistical analyses, sequence clustering, and figure generation are available from the corresponding author upon reasonable request.

References

1. Antimicrobial Resistance Collaborators. Global burden of bacterial antimicrobial resistance in 2019: a systematic analysis. *Lancet* 399, 629–655 (2022). https://doi.org/10.1016/S0140-6736(21)02724-0
2. One Health High-Level Expert Panel (OHHLEP) *et al.* One Health: A new definition for a sustainable and healthy future. *PLoS Pathog* 18, e1010537 (2022). https://doi.org/10.1371/journal.ppat.1010537
3. Hao, H. *et al.* Benefits and risks of antimicrobial use in food-producing animals. *Front Microbiol* 5, 288 (2014). https://doi.org/10.3389/fmicb.2014.00288
4. Ruegg, P. L. A 100-Year Review: Mastitis detection, management, and prevention. *J Dairy Sci* 100, 10381–10397 (2017). https://doi.org/10.3168/jds.2017-13023

5. Vezina, B. *et al.* Sequence characterisation and novel insights into bovine mastitis-associated *Streptococcus uberis* in dairy herds. *Sci Rep* 11, 3046 (2021). https://doi.org/10.1038/s41598-021-82357-3
6. Heikkila, A. M., Liski, E., Pyorala, S. & Taponen, S. Pathogen-specific production losses in bovine mastitis. *J Dairy Sci* 101, 9493–9504 (2018). https://doi.org/10.3168/jds.2018-14824
7. Silva, N. C. C., Yang, Y., Rodrigues, M. X., Tomazi, T. & Bicalho, R. C. Whole-genome sequencing reveals high genetic diversity of *Streptococcus uberis* isolated from cows with mastitis. *BMC Vet Res* 17, 321 (2021). https://doi.org/10.1186/s12917-021-03031-4
8. McCubbin, K. D. *et al.* Invited review: Selective use of antimicrobials in dairy cattle at drying-off. *J Dairy Sci* 105, 7161–7189 (2022). https://doi.org/10.3168/jds.2021-21455
9. Tsuyuki, Y. *et al.* Antimicrobial resistance patterns of *Streptococcus uberis* isolates from bovine milk in Chiba prefecture, Japan: association between multidrug resistance and clonal complex 996. *J Vet Med Sci* 86, 468–473 (2024). https://doi.org/10.1292/jvms.23-0526
10. Partridge, S. R., Kwong, S. M., Firth, N. & Jensen, S. O. Mobile Genetic Elements Associated with Antimicrobial Resistance. *Clin Microbiol Rev* 31, e00088-17 (2018). https://doi.org/10.1128/CMR.00088-17
11. Arnold, B. J., Huang, I. T. & Hanage, W. P. Horizontal gene transfer and adaptive evolution in bacteria. *Nat Rev Microbiol* 20, 206–218 (2022). https://doi.org/10.1038/s41579-021-00650-4
12. Johnson, C. M. & Grossman, A. D. Integrative and Conjugative Elements (ICEs): What They Do and How They Work. *Annu Rev Genet* 49, 577–601 (2015). https://doi.org/10.1146/annurev-genet-112414-055018
13. Lao, J. *et al.* ICEscreen: a tool to detect *Firmicute* ICEs and IMEs, isolated or enclosed in composite structures. *NAR Genomics and Bioinformatics* 4, lqac079 (2022). https://doi.org/10.1093/nargab/lqac079
14. Pal, C., Bengtsson-Palme, J., Kristiansson, E. & Larsson, D. G. Co-occurrence of resistance genes to antibiotics, biocides and metals reveals novel insights into their co-selection potential. *BMC Genomics* 16, 964 (2015). https://doi.org/10.1186/s12864-015-2153-5
15. Haenni, M. *et al.* Diversity and mobility of integrative and conjugative elements in bovine isolates of *Streptococcus agalactiae*, *S. dysgalactiae* subsp. *dysgalactiae*, and *S. uberis*. *Appl Environ Microbiol* 76, 7957–7965 (2010). https://doi.org/10.1128/AEM.00805-10
16. Maeda, T., Tsuyuki, Y., Yoshida, H., Goto, M. & Takahashi, T. Characterization of integrative and conjugative elements carrying *erm(B)* and *tet(O)* resistance determinants in *Streptococcus uberis* isolates from bovine milk in Chiba prefecture, Japan: CompArative GEne cluster analysis toolbox with ICEfinder. *BMC Res Notes* 17, 377 (2024). https://doi.org/10.1186/s13104-024-07065-3
17. Hosoi, Y. *et al.* Antimicrobial Use in the Animal Sector in Japan from 2011 to 2022. *Antibiotics (Basel)* 13, 1204 (2024). https://doi.org/10.3390/antibiotics13121204
18. Kikuchi, M. *et al.* Evaluating the antimicrobial use on dairy farms in Chiba Prefecture in Japan using the antimicrobial treatment incidence, an indicator based on Japanese defined daily doses from

2014–2016. *J Vet Med Sci* 84, 1164–1174 (2022). https://doi.org/10.1292/jvms.21-0672

19. Wirawan, R. E., Klesse, N. A., Jack, R. W. & Tagg, J. R. Molecular and genetic characterization of a novel nisin variant produced by *Streptococcus uberis*. *Appl Environ Microbiol* 72, 1148–1156 (2006). https://doi.org/10.1128/AEM.72.2.1148-1156.2006
20. Gu, Q. *et al.* Type II and IV toxin-antitoxin systems coordinately stabilize the integrative and conjugative element of the ICESa2603 family conferring multiple drug resistance in *Streptococcus suis*. *PLoS Pathog* 20, e1012169 (2024). https://doi.org/10.1371/journal.ppat.1012169
21. de Jong, E. *et al.* Invited review: Selective treatment of clinical mastitis in dairy cattle. *J Dairy Sci* 106, 3761–3778 (2023). https://doi.org/10.3168/jds.2022-22826
22. Roberts, A. P. & Mullany, P. Tn916-like genetic elements: a diverse group of modular mobile elements conferring antibiotic resistance. *FEMS Microbiol Rev* 35, 856–871 (2011). https://doi.org/10.1111/j.1574-6976.2011.00283.x
23. Wee, B. A., Muloi, D. M. & van Bunnik, B. A. D. Quantifying the transmission of antimicrobial resistance at the human and livestock interface with genomics. *Clin Microbiol Infect* 26, 1612–1616 (2020). https://doi.org/10.1016/j.cmi.2020.09.019
24. Muloi, D. M. *et al.* Exploiting genomics for antimicrobial resistance surveillance at One Health interfaces. *Lancet Microbe* 4, e1056–e1062 (2023). https://doi.org/10.1016/S2666-5247(23)00284-7
25. Crestani, C. *et al.* The fall and rise of group B *Streptococcus* in dairy cattle: reintroduction due to human-to-cattle host jumps? *Microb Genom* 7, 000648 (2021). https://doi.org/10.1099/mgen.0.000648
26. Malachowa, N. & DeLeo, F. R. Mobile genetic elements of *Staphylococcus aureus*. *Cell Mol Life Sci* 67, 3057–3071 (2010). https://doi.org/10.1007/s00018-010-0389-4
27. Prevention of Group B Streptococcal Early-Onset Disease in Newborns: ACOG Committee Opinion, Number 797. *Obstet Gynecol* 135, e51–e72 (2020). https://doi.org/10.1097/AOG.0000000000003668
28. Gygax, S. E. *et al.* Erythromycin and clindamycin resistance in group B streptococcal clinical isolates. *Antimicrob Agents Chemother* 50, 1875–1877 (2006). https://doi.org/10.1128/AAC.50.5.1875-1877.2006
29. Watt, A. E. *et al.* Parameters for one health genomic surveillance of *Escherichia coli* from Australia. *Nat Commun* 16, 17 (2025). https://doi.org/10.1038/s41467-024-55103-2
30. Matsui, H. *et al.* Use of Recombinant Endolysin to Improve Accuracy of Group B *Streptococcus* Tests. *Microbiology Spectrum* 9, e00077-21 (2021). https://doi.org/10.1128/spectrum.00077-21
31. Chen, S., Zhou, Y., Chen, Y. & Gu, J. fastp: an ultra-fast all-in-one FASTQ preprocessor. *Bioinformatics (Oxford, England)* 34, i884–i890 (2018). https://doi.org/10.1093/bioinformatics/bty560
32. Prjibelski, A., Antipov, D., Meleshko, D., Lapidus, A. & Korobeynikov, A. Using SPAdes De Novo Assembler. *Current Protocols in Bioinformatics* 70, e102 (2020). https://doi.org/10.1002/cpbi.102

33. Mikheenko, A., Prjibelski, A., Saveliev, V., Antipov, D. & Gurevich, A. Versatile genome assembly evaluation with QUAST-LG. *Bioinformatics (Oxford, England)* 34, i142–i150 (2018). https://doi.org/10.1093/bioinformatics/bty266
34. Blin, K. ncbi-genome-download v. 0.3.3 (Zenodo, 2023). https://doi.org/10.5281/zenodo.8192486
35. Seemann, T. Prokka: rapid prokaryotic genome annotation. *Bioinformatics (Oxford, England)* 30, 2068–2069 (2014). https://doi.org/10.1093/bioinformatics/btu153
36. Page, A. J. *et al.* Roary: rapid large-scale prokaryote pan genome analysis. *Bioinformatics (Oxford, England)* 31, 3691–3693 (2015). https://doi.org/10.1093/bioinformatics/btv421
37. Katoh, K. & Standley, D. M. MAFFT multiple sequence alignment software version 7: improvements in performance and usability. *Mol Biol Evol* 30, 772–780 (2013). https://doi.org/10.1093/molbev/mst010
38. Price, M. N., Dehal, P. S. & Arkin, A. P. FastTree 2–approximately maximum-likelihood trees for large alignments. *PLoS One* 5, e9490 (2010). https://doi.org/10.1371/journal.pone.0009490
39. Letunic, I. & Bork, P. Interactive Tree of Life (iTOL) v6: recent updates to the phylogenetic tree display and annotation tool. *Nucleic Acids Research* 52, W78–W82 (2024). https://doi.org/10.1093/nar/gkae268
40. Feldgarden, M. *et al.* AMRFinderPlus and the Reference Gene Catalog facilitate examination of the genomic links among antimicrobial resistance, stress response, and virulence. *Scientific Reports* 11, 12728 (2021). https://doi.org/10.1038/s41598-021-91456-0
41. R Core Team. R: A Language and Environment for Statistical Computing (R Foundation for Statistical Computing, Vienna, Austria, 2025).
42. Kolde, R. pheatmap: Pretty Heatmaps v. 1.0.13 (Comprehensive R Archive Network (CRAN), 2025). https://doi.org/10.32614/CRAN.package.pheatmap
43. De Caceres, M. & Legendre, P. Associations between species and groups of sites: indices and statistical inference. *Ecology* 90, 3566–3574 (2009). https://doi.org/10.1890/08-1823.1
44. Seemann, T. mlst: Scan contig files against PubMLST typing schemes v. 2.23.0 (GitHub, 2022).
45. Jolley, K. A., Bray, J. E. & Maiden, M. C. J. Open-access bacterial population genomics: BIGSdb software, the PubMLST.org website and their applications. *Wellcome Open Res* 3, 124 (2018). https://doi.org/10.12688/wellcomeopenres.14826.1
46. Nascimento, M. *et al.* PHYLOViZ 2.0: providing scalable data integration and visualization for multiple phylogenetic inference methods. *Bioinformatics (Oxford, England)* 33, 128–129 (2017). https://doi.org/10.1093/bioinformatics/btw582
47. Clinical and Laboratory Standards Institute. Performance Standards for Antimicrobial Disk and Dilution Susceptibility Tests for Bacteria Isolated From Animals. 7th ed. CLSI supplement VET01S (Clinical and Laboratory Standards Institute, 2024).
48. Monistero, V. *et al.* Genotyping and Antimicrobial Susceptibility Profiling of *Streptococcus uberis* Isolated from a Clinical Bovine Mastitis Outbreak in a Dairy Farm. *Antibiotics (Basel)* 10, 644 (2021).

https://doi.org/10.3390/antibiotics10060644

49. Zouharova, M., Nedbalcova, K., Matiaskova, K., Slama, P. & Matiasovic, J. Antimicrobial Susceptibility and Resistance Genes in *Streptococcus uberis* Isolated from Bovine Mastitis in the Czech Republic. *Antibiotics (Basel)* 12, 1527 (2023). https://doi.org/10.3390/antibiotics12101527
50. Clinical and Laboratory Standards Institute. Performance Standards for Antimicrobial Susceptibility Testing. 36th ed. CLSI supplement M100 (Clinical and Laboratory Standards Institute, 2026).
51. Paradis, E. & Schliep, K. ape 5.0: an environment for modern phylogenetics and evolutionary analyses in R. *Bioinformatics (Oxford, England)* 35, 526–528 (2019). https://doi.org/10.1093/bioinformatics/bty633
52. Oksanen, J. *et al.* vegan: Community Ecology Package v. 2.7-5 (Comprehensive R Archive Network (CRAN), 2026). https://doi.org/10.32614/CRAN.package.vegan
53. Bellanger, X. *et al.* Conjugative transfer of the integrative conjugative elements ICESt1 and ICESt3 from *Streptococcus thermophilus*. *J Bacteriol* 191, 2764–2775 (2009). https://doi.org/10.1128/JB.01412-08
54. Camacho, C. *et al.* BLAST+: architecture and applications. *BMC Bioinformatics* 10, 421 (2009). https://doi.org/10.1186/1471-2105-10-421
55. Katz, L. S. *et al.* Mashtree: a rapid comparison of whole genome sequence files. *Journal of Open Source Software* 4, 1762 (2019). https://doi.org/10.21105/joss.01762
56. Wickham, H., François, R., Henry, L., Müller, K. & Vaughan, D. dplyr: A Grammar of Data Manipulation v. 1.2.1 (R package, 2026).
57. Yang, M., Derbyshire, M. K., Yamashita, R. A. & Marchler-Bauer, A. NCBI's Conserved Domain Database and Tools for Protein Domain Analysis. *Current Protocols in Bioinformatics* 69, e90 (2020). https://doi.org/10.1002/cpbi.90
58. Borowiec, M. L. AMAS: a fast tool for alignment manipulation and computing of summary statistics. *PeerJ* 4, e1660 (2016). https://doi.org/10.7717/peerj.1660
59. Wong, T. K. F. *et al.* IQ-TREE 3: phylogenomic inference software using complex evolutionary models. *Molecular Biology and Evolution* 43, msag117 (2026). https://doi.org/10.1093/molbev/msag117
60. Sullivan, M. J., Petty, N. K. & Beatson, S. A. Easyfig: a genome comparison visualizer. *Bioinformatics (Oxford, England)* 27, 1009–1010 (2011). https://doi.org/10.1093/bioinformatics/btr039

Figures

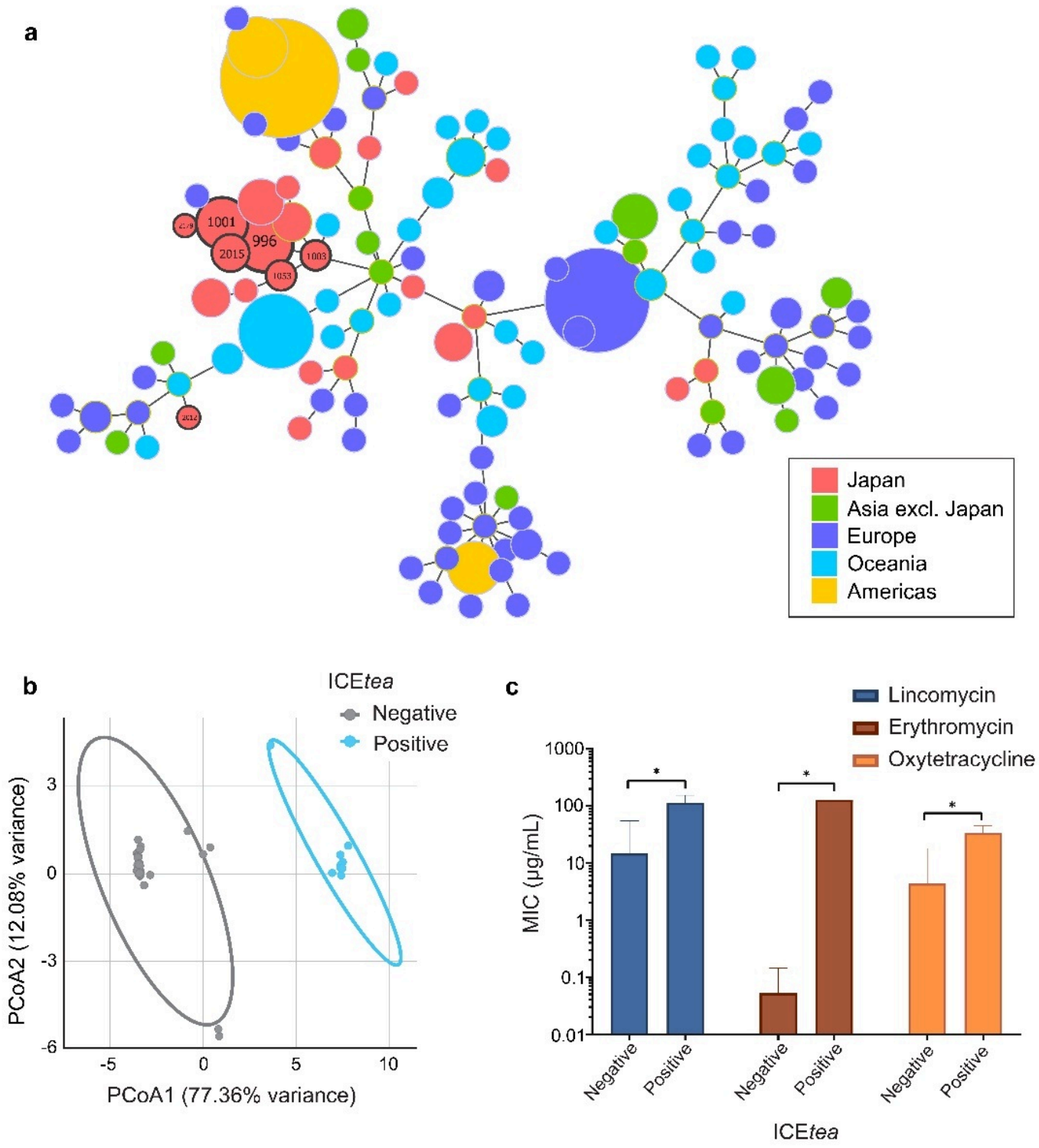


Figure 1

Genomic and antimicrobial susceptibility features of ICE*tea*-positive *S. uberis* isolates in Japan. a ICE*tea*-positive *S. uberis* isolates mapped onto a goeBURST minimum spanning tree based on multilocus sequence typing. Node colors indicate geographic regions: Japan, Asia excluding Japan, Europe, Oceania, and the Americas. Node size is proportional to the number of isolates represented by each sequence type (ST). Black-bordered nodes indicate STs containing ICE*tea*-positive isolates. Numbers

within nodes indicate the corresponding STs. **b** PCoA based on $\log_2$-transformed MIC profiles. ICE*tea*-positive and ICE*tea*-negative isolates are indicated separately. Ellipses represent 95% confidence regions for each group. Environmental vector fitting identified lincomycin, erythromycin, and oxytetracycline as the antimicrobial agents most strongly associated with variation in the ordination (R^2 = 0.98, 0.95, and 0.69, respectively; P = 0.001 for all; Supplementary Table S5). **c** Comparison of MICs for lincomycin, erythromycin, and oxytetracycline between ICE*tea*-positive and ICE*tea*-negative isolates. The asterisk (*) indicates statistically significant differences between groups (two-sided Mann–Whitney *U* test with Benjamini–Hochberg FDR correction; FDR-adjusted P < 0.001). Bars and error bars indicate the mean and SD, respectively.

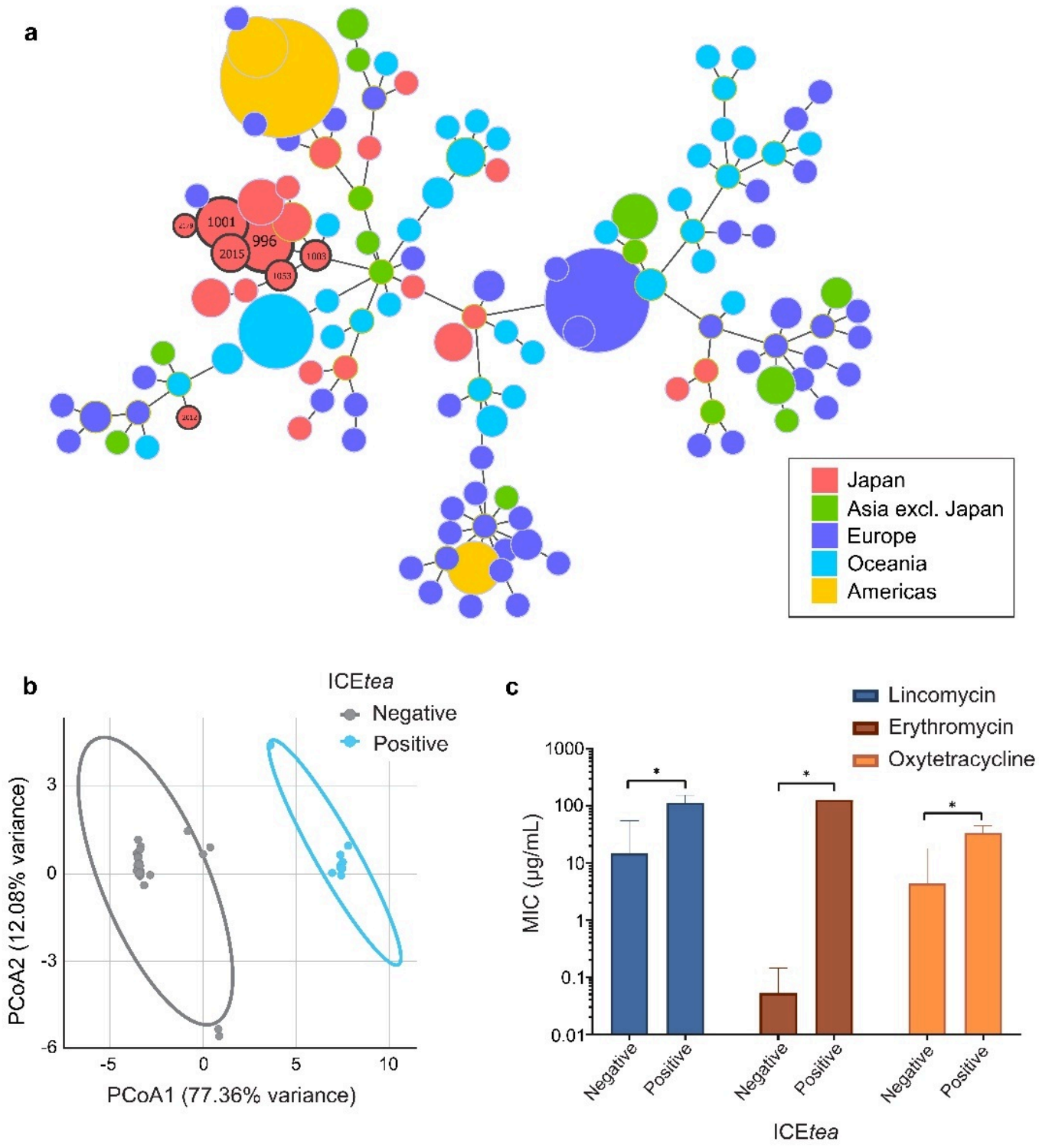


Figure 1

Genomic and antimicrobial susceptibility features of ICE*tea*-positive *S. uberis* isolates in Japan. a ICE*tea*-positive *S. uberis* isolates mapped onto a goeBURST minimum spanning tree based on multilocus sequence typing. Node colors indicate geographic regions: Japan, Asia excluding Japan, Europe, Oceania, and the Americas. Node size is proportional to the number of isolates represented by each sequence type (ST). Black-bordered nodes indicate STs containing ICE*tea*-positive isolates. Numbers

within nodes indicate the corresponding STs. **b** PCoA based on $\log_2$-transformed MIC profiles. ICE*tea*-positive and ICE*tea*-negative isolates are indicated separately. Ellipses represent 95% confidence regions for each group. Environmental vector fitting identified lincomycin, erythromycin, and oxytetracycline as the antimicrobial agents most strongly associated with variation in the ordination (R^2 = 0.98, 0.95, and 0.69, respectively; P = 0.001 for all; Supplementary Table S5). **c** Comparison of MICs for lincomycin, erythromycin, and oxytetracycline between ICE*tea*-positive and ICE*tea*-negative isolates. The asterisk (*) indicates statistically significant differences between groups (two-sided Mann–Whitney *U* test with Benjamini–Hochberg FDR correction; FDR-adjusted P < 0.001). Bars and error bars indicate the mean and SD, respectively.

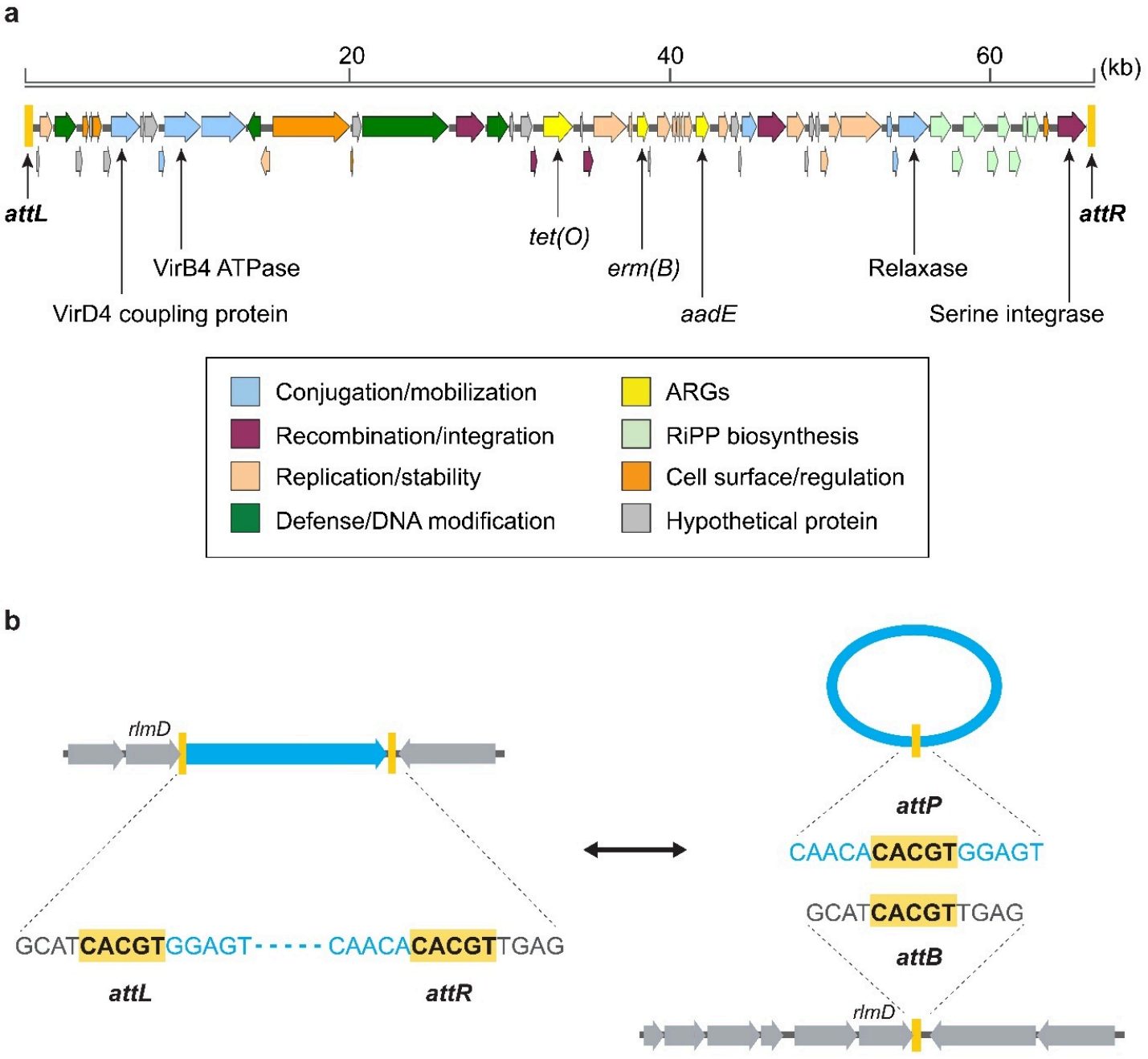


Figure 2

Genetic organization and attachment-site structure of ICE*tea*. a Genetic organization of ICE*tea*in *S. uberis*. Predicted coding sequences are shown as arrows, with arrowheads indicating the direction of transcription. Genes are color-coded according to predicted functional categories. The “RiPP biosynthesis” category includes genes associated with the lantibiotic biosynthesis, regulation, transport, and immunity discussed in the text. The left and right attachment sites of the integrated element are indicated as *attL* and *attR*, respectively. Representative genes involved in conjugation, recombination/integration, and AMR are annotated. The ARGs *tet(O)*, *erm(B)*, and *aadE* are indicated. The scale bar at the top indicates nucleotide positions along the ICE*tea* sequence in kilobases. **b**Analysis of the ICE*tea* integration site. On the left, a schematic diagram of the integrated form of ICE*tea* is shown. The conserved 5-bp core sequence shared by *attL* and *attR* (5'-CACGT-3') is highlighted in yellow. ICE*tea* was integrated at the 3' end of the *rlmD*gene. On the right, schematic diagrams of the circularized form of ICE*tea*and the bacterial genome are shown. The conserved 5-bp core sequence shared by *attP*and *attB* (5'-CACGT-3') is highlighted in yellow.

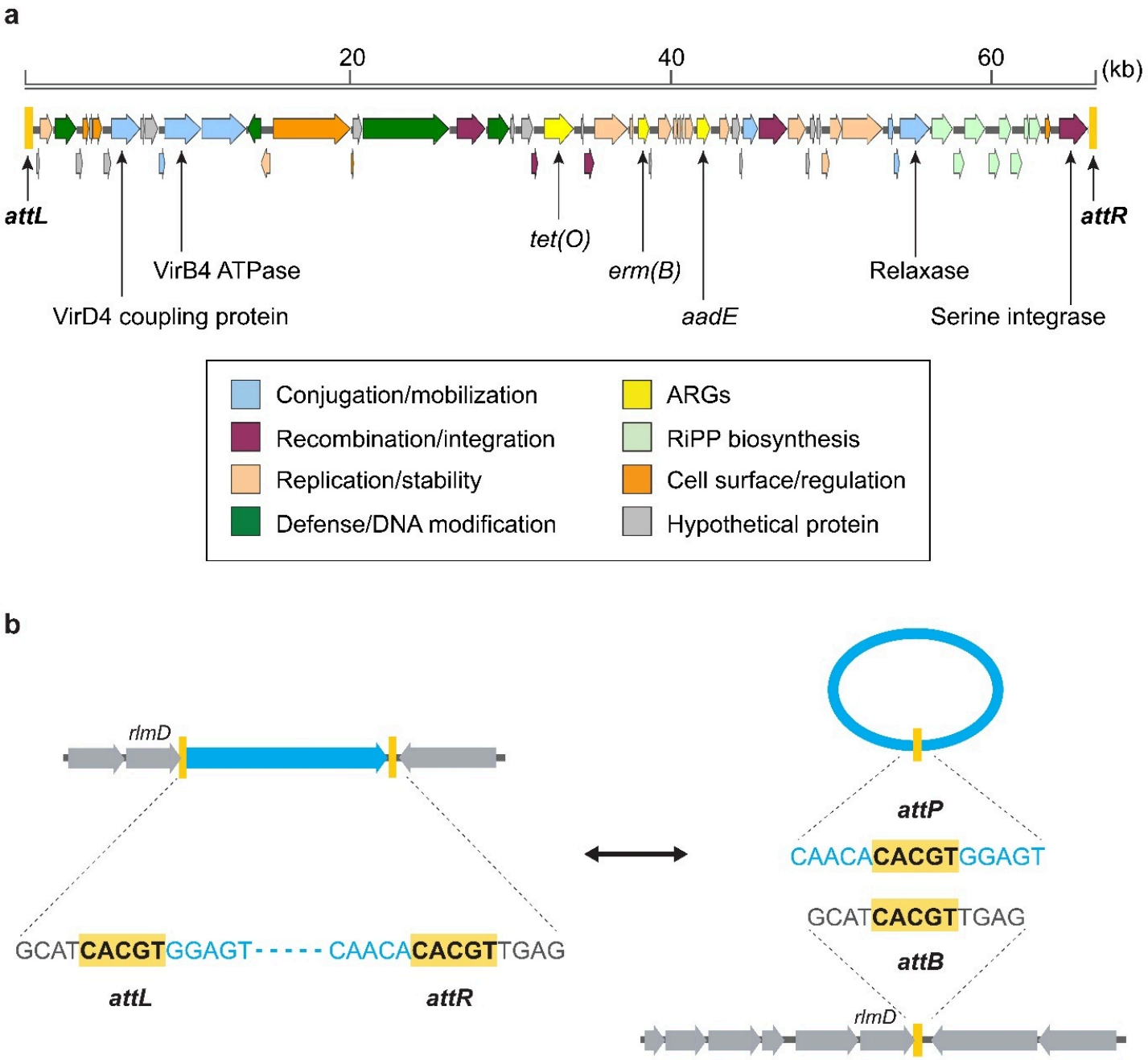


Figure 2

Genetic organization and attachment-site structure of ICE*tea*. a Genetic organization of ICE*tea*in *S. uberis*. Predicted coding sequences are shown as arrows, with arrowheads indicating the direction of transcription. Genes are color-coded according to predicted functional categories. The “RiPP biosynthesis” category includes genes associated with the lantibiotic biosynthesis, regulation, transport, and immunity discussed in the text. The left and right attachment sites of the integrated element are indicated as *attL* and *attR*, respectively. Representative genes involved in conjugation, recombination/integration, and AMR are annotated. The ARGs *tet(O)*, *erm(B)*, and *aadE* are indicated. The

scale bar at the top indicates nucleotide positions along the ICE*tea* sequence in kilobases. **b**Analysis of the ICE*tea* integration site. On the left, a schematic diagram of the integrated form of ICE*tea* is shown. The conserved 5-bp core sequence shared by *attL* and *attR* (5'-CACGT-3') is highlighted in yellow. ICE*tea* was integrated at the 3' end of the *rlmD*gene. On the right, schematic diagrams of the circularized form of ICE*tea*and the bacterial genome are shown. The conserved 5-bp core sequence shared by *attP*and *attB* (5'-CACGT-3') is highlighted in yellow.

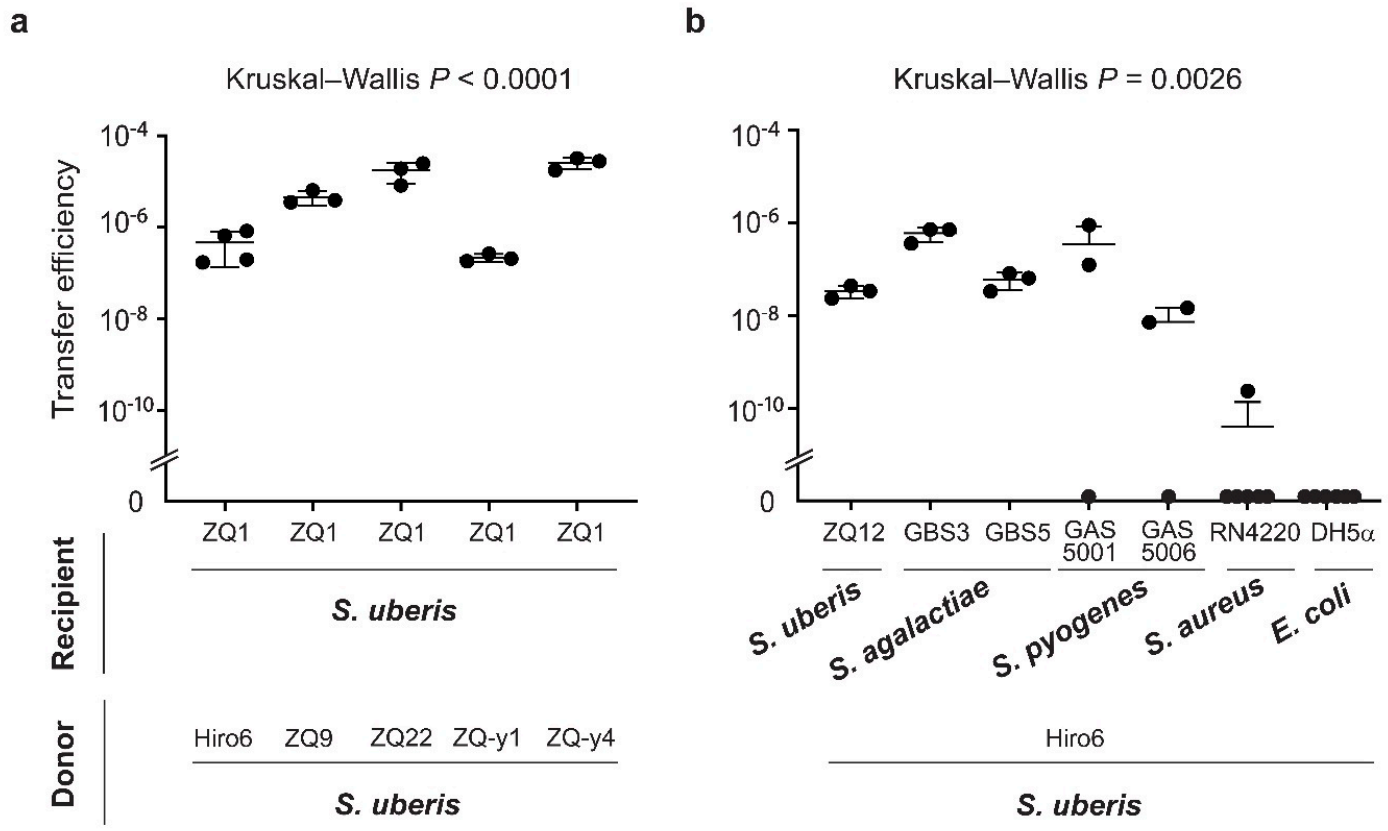


Figure 3

Experimental conjugative transfer of ICE*tea* among *S. uberis* strains and to other bacterial species. Horizontal bars indicate means, vertical error bars indicate SD, and individual data points represent biologically independent replicates (n ≥ 3). Transfer efficiency is expressed as the number of transconjugants per recipient and plotted on a logarithmic scale. Positive transfer efficiencies are plotted on a logarithmic scale; zero values, corresponding to no detectable transconjugants, are displayed separately at 0 below the axis break. Overall differences among donor–recipient combinations were assessed using the Kruskal–Wallis test followed by Dunn's multiple comparisons test. **a** Transfer efficiencies of ICE*tea* among *S. uberis*strains. *S. uberis* strains Hiro6, ZQ9, ZQ22, ZQ-y1, and ZQ-y4 were used as donors, and *S. uberis* strain ZQ1 was used as the recipient. The overall difference among donor–recipient combinations was significant (H= 13.11, P < 0.0001); however, no pairwise comparison was significant in Dunn's multiple comparisons test. **b** Transfer efficiencies of ICE*tea*from *S. uberis* to other

bacterial species. *S. uberis* strain Hiro6 was used as the donor. *S. uberis* strain ZQ12, *S. agalactiae*strains GBS3 and GBS5, *S. pyogenes* strains GAS5001 and GAS5006, *S. aureus* strain RN4220, and *E. coli* strain DH5a were used as recipients. The overall difference among recipient strains was significant ($H = 20.13$, $P = 0.0026$). Dunn's multiple comparisons test identified significant differences between GBS3 and RN4220 (adjusted $P = 0.0308$) and between GBS3 and DH5a (adjusted $P = 0.0141$). No transconjugants were obtained with *E. coli* DH5a.

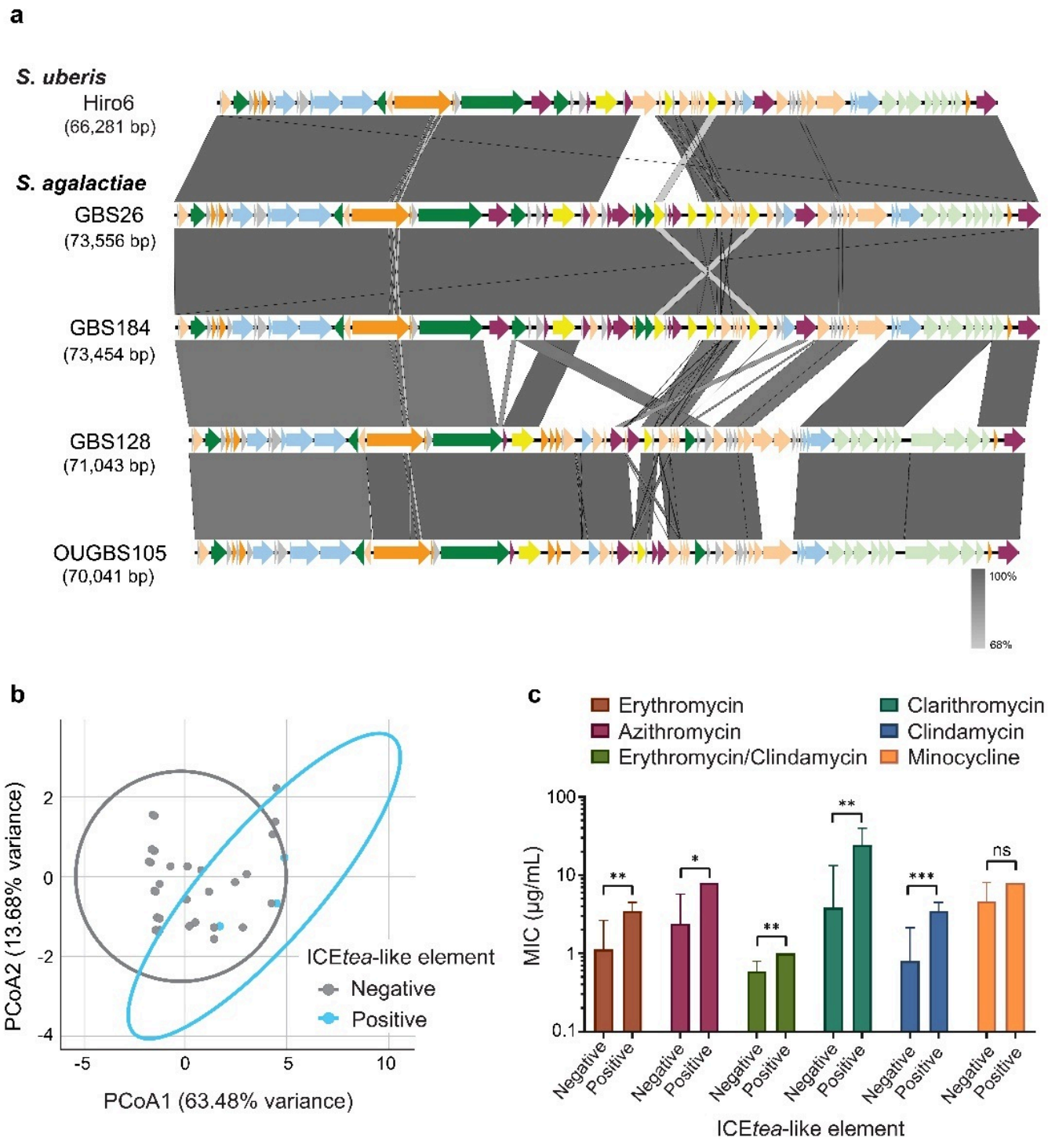


Figure 4

ICE*tea*-like elements and antimicrobial susceptibility profiles in human-derived *S. agalactiae* isolates. a Comparative genetic organization of ICE*tea*-like elements detected in four human-derived *S. agalactiae* isolates from Japan. ICE*tea* from *S. uberis* is shown as the reference. Arrows indicate predicted coding sequences and their transcriptional orientation, colored by functional category, as in Fig. 2a. Gray shading indicates nucleotide identity (68%–100%). Insertions and partial deletions were observed in the *S. agalactiae* ICE*tea*-like elements relative to *S. uberis* ICE*tea*. **b** PCoA based on $\log_2$-transformed MIC profiles of 67 human-derived *S. agalactiae* isolates, including four ICE*tea*-like element-positive and 63 negative isolates. Environmental vector fitting was performed for 19 antimicrobial agents to identify those associated with variation in the ordination. Ellipses represent 95% confidence regions for each group. **c** Comparison of MICs for selected antimicrobial agents between ICE*tea*-like element-positive and -negative *S. agalactiae* isolates. Asterisks indicate statistically significant differences between groups (two-sided Mann–Whitney *U* test with Benjamini–Hochberg FDR correction): * FDR-adjusted $P < 0.05$, ** FDR-adjusted $P < 0.01$, *** FDR-adjusted $P < 0.001$; ns, not significant. Bars and error bars indicate the mean and SD, respectively.

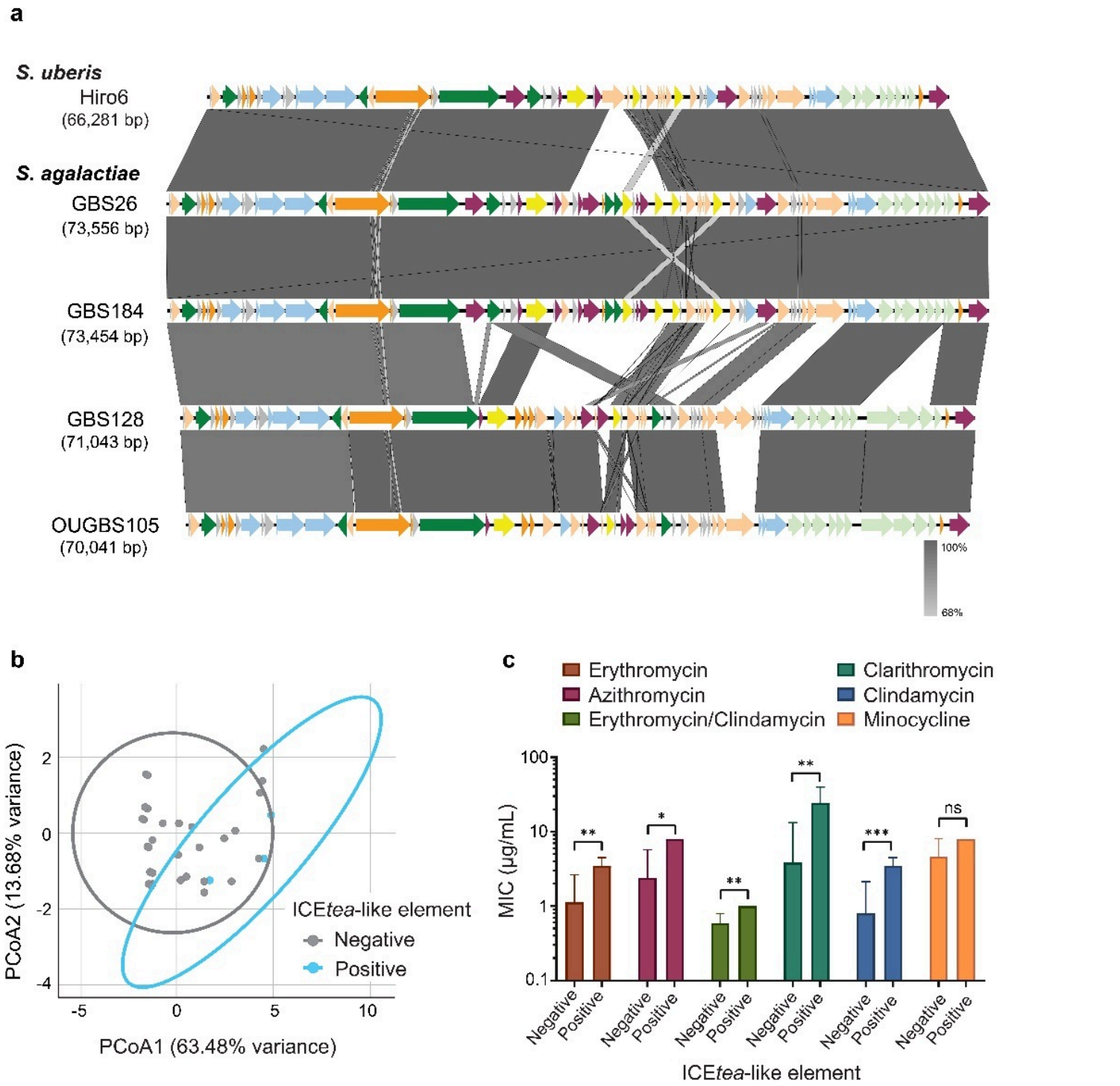


Figure 4

ICE*tea*-like elements and antimicrobial susceptibility profiles in human-derived *S. agalactiae* isolates. a Comparative genetic organization of ICE*tea*-like elements detected in four human-derived *S. agalactiae* isolates from Japan. ICE*tea* from *S. uberis* is shown as the reference. Arrows indicate predicted coding sequences and their transcriptional orientation, colored by functional category, as in Fig. 2a. Gray shading indicates nucleotide identity (68%–100%). Insertions and partial deletions were observed in the

S. agalactiae ICE*tea*-like elements relative to *S. uberis* ICE*tea*. **b** PCoA based on log_2-transformed MIC profiles of 67 human-derived *S. agalactiae* isolates, including four ICE*tea*-like element-positive and 63 negative isolates. Environmental vector fitting was performed for 19 antimicrobial agents to identify those associated with variation in the ordination. Ellipses represent 95% confidence regions for each group. **c** Comparison of MICs for selected antimicrobial agents between ICE*tea*-like element-positive and -negative *S. agalactiae* isolates. Asterisks indicate statistically significant differences between groups (two-sided Mann–Whitney *U* test with Benjamini–Hochberg FDR correction): * FDR-adjusted $P < 0.05$, ** FDR-adjusted $P < 0.01$, *** FDR-adjusted $P < 0.001$; ns, not significant. Bars and error bars indicate the mean and SD, respectively.

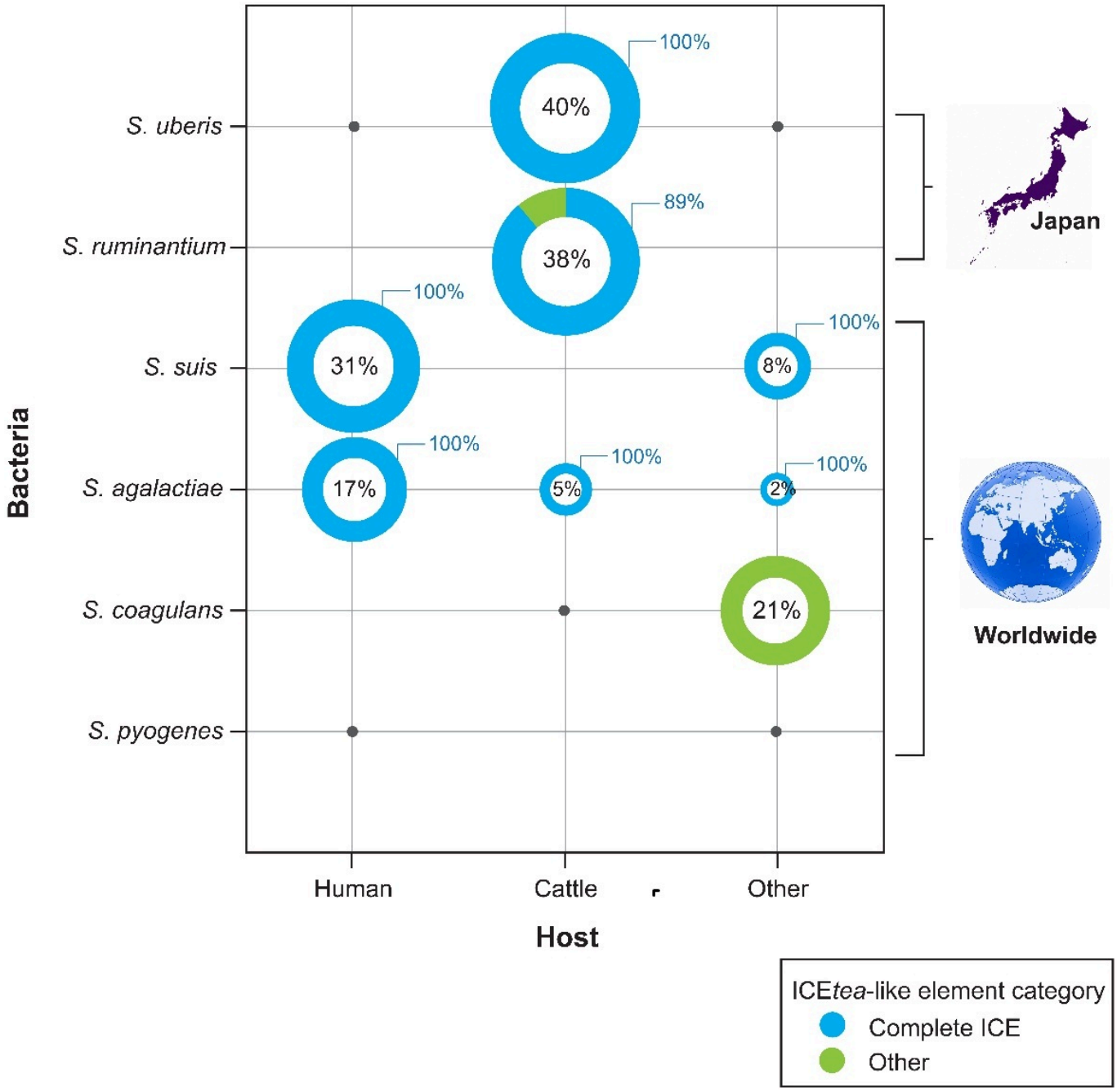


Figure 5

Distribution of ICE*tea*-like elements across Gram-positive bacterial taxa and host origins. The comparative distribution analysis included 1,079 genomes, comprising 1,042 publicly available RefSeq genomes from selected streptococcal and staphylococcal species and 37 *S. uberis* genomes newly sequenced in this study. The four *S. agalactiae* genomes sequenced after PCR-positive selection were excluded from proportion calculations but retained for subsequent phylogenetic and structural analyses. The bubble size and percentage shown at the center of each bubble indicate the proportion of genomes carrying ICE*tea*-like elements within each species–host group. Donut segments indicate ICEscreen-based classifications: blue, ICE*tea*-like elements predicted as “Complete ICE”; green, elements classified as “Other.” External blue labels indicate the proportion of detected ICE*tea*-like elements classified as “Complete ICE” within each group. Small gray dots indicate species–host groups for which genome data were available, but no ICE*tea*-like elements were detected. Blank positions indicate species–host combinations for which no genome data were available in the analyzed dataset. The distributions of ICE*tea*-like elements are shown for *S. uberis* and *S. ruminantium* in Japan, and for *S. suis*, *S. agalactiae*, *S. coagulans*, and *S. pyogenes* worldwide.

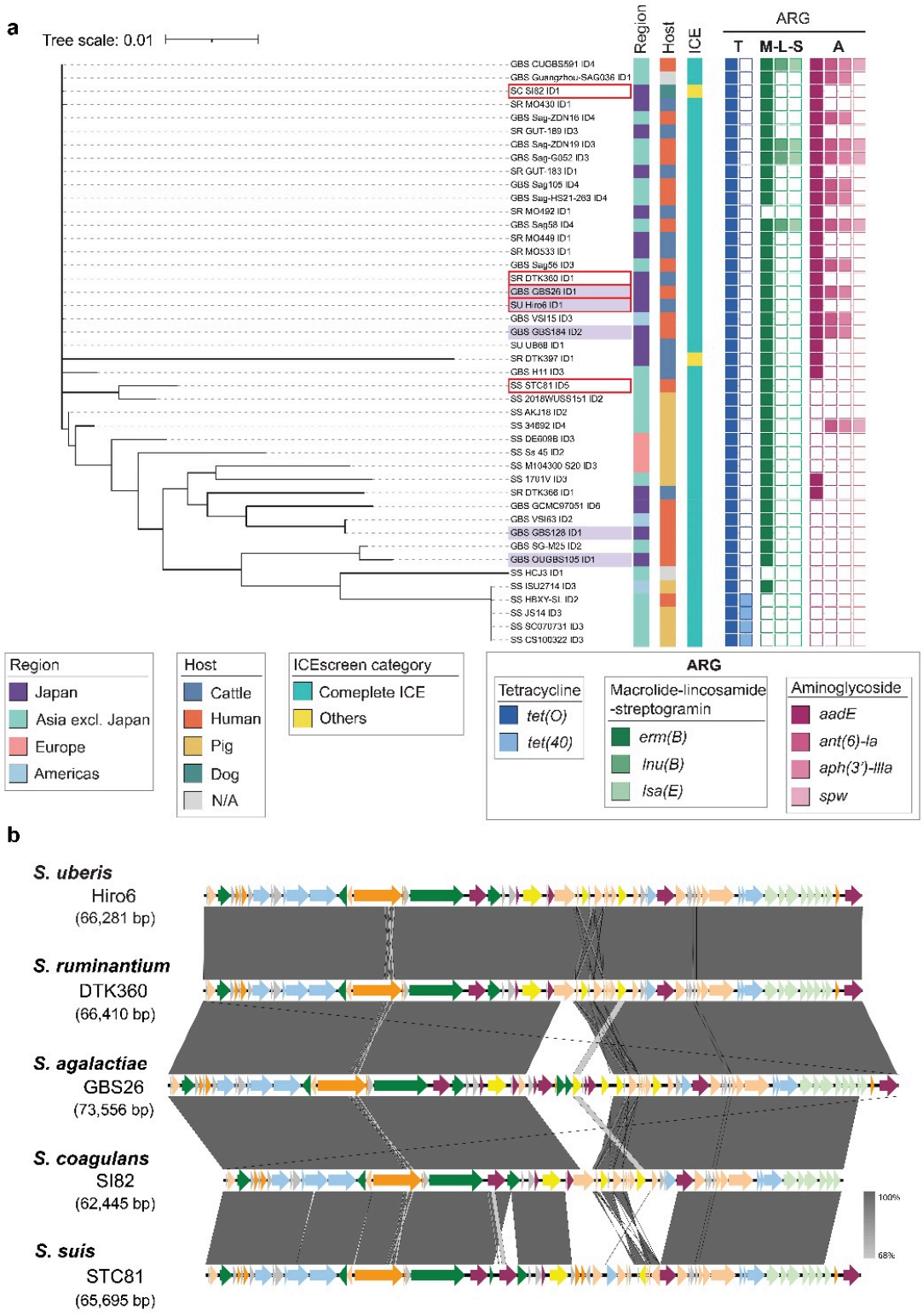


Figure 6

Phylogenetic and structural comparison of ICE*tea*-like elements. a Maximum-likelihood phylogenetic tree of 44 representative ICE*tea*-like elements based on seven conserved ICE-associated genes: relaxase, VirD4, VirB4, MobC, Tn5252_Orf10, TnpV, and PrgI. Metadata tracks indicate geographic region, host origin, ICEscreen category, and ARG content. ARG classes are abbreviated as T, tetracycline; M-L-S, macrolide–lincosamide–streptogramin; and A, aminoglycoside. SU, *S. uberis*; SR, *S. ruminantium*; GBS, *S.*

agalactiae; SC, *S. coagulans*; SS, *S. suis*. Strain names highlighted in purple indicate strains sequenced in this study; red boxes indicate elements selected for panel **b** based on their phylogenetic proximity to *S. uberis* ICE*tea*. **b** Comparative genetic organization of representative ICE*tea*-like elements. Arrows indicate coding sequences and transcriptional orientation, with functional categories colored as in Fig. 2a. Gray shading indicates nucleotide identity (68%–100%).

Supplementary Files

This is a list of supplementary files associated with this preprint. Click to download.

- Supplementarydata.pdf